Design and Fabrication of Silver Deposited TiO_2 Nanotubes: Antibacterial Applications

Parsoua Abedini Sohi

A Thesis

In

The Department

of

Electrical and Computer Engineering

Presented in Partial Fulfillment of Requirements

For the Degree of Master of Applied Science

(Electrical & Computer Engineering) at

Concordia University

Montreal, Quebec, Canada

July 2013

CONCORDIA UNIVERSITY

SCHOOL OF GRADUATE STUDIES

This is to certify that the thesis prepared

By: Parsoua Abedini Sohi

Entitled: "Design and Fabrication of Silver Deposited TiO_2 Nanotubes: Antibacterial Applications"

and submitted in partial fulfillment of the requirements for the degree of

Master of Applied Science

Complies with the regulations of this University and meets the accepted standards with respect to originality and quality.

Signed by the final examining committee:

_____ Chair

Dr. M. Z. Kabir

_____ Examiner, External

Dr. L. Varin (Biology) To the Program

_____ Examiner

Dr. I. Stateikina

_____ Supervisor

Dr. M. Kahrizi

Approved by: _____

Dr. W. E. Lynch, Chair

Department of Electrical and Computer Engineering

_____20_____ _____

Dr. C. W. Trueman

Interim Dean, Faculty of Engineering and Computer Science

ABSTRACT

Design and Fabrication of Silver Deposited TiO_2 Nanotubes: Antibacterial Applications

Parsoua Abedini Sohi

Clean water is one of the most challenging issues facing humanity today resulting in widespread research on new water purification and disinfection techniques emphasizing on optimized energy consumption. Nanotechnology has significantly contributed to the lowering the cost of eco-friendly water disinfecting processes. Among many materials in this study TiO2 nanotubes with 90-100 nm pore diameter were synthesized using anodization method in an organic electrolyte containing fluoride ions. Deposition of Silver (Ag) on the large-surface TiO2 nanotubes showed significant antibacterial activity. To improve the uniformity of silver deposition a reductive doping was performed to increase the conductivity of the TiO2 nanotubes. Silver deposition was performed in a three-electrode electrodeposition cell using a cyanide-based silver electrolyte. Characterization of the films using scanning electron microscopy (SEM) and energy dispersive X-ray spectroscopy (EDX) confirmed the deposition of Ag onto the TiO2 porous layer. Liquid medium test under light illumination followed by serial dilutions resulted in perfect photo biocide efficiency of the immobilized Ag/TiO2 against *E. Coli* which is an emerging cause of food borne and waterborne illnesses.

Acknowledgements

I would like to express my great appreciation to my supervisor, Dr. Mojtaba Kahrizi for his guidance, encouragement, and suggestions during my study.

I would like to express my deep gratitude to Dr. Luc Varin for his valuable scientific advises regarding the practical application of my research project.

I would also like to extend my thanks to my colleague, Mahmoud Amouzgar, for his patient guidance and important assistance during this research.

I am also thankful to my supervisory committee for their review my thesis and providing constructive feedback.

I would like to thank family most importantly my dear husband, Nima, for his patience, understanding and love during these years, our parents Amir and Mojgan, Nasrin and Kamal,for their unforgettable encouragement and supports.

CONTENTS

LIST OF FIGURES

LIST OF TABLES

LIST OF ACRONYMS

AAO	Anodized Aluminum Oxide
AgNO3	Silver Nitrate
Ag	Silver
°C	Celsius
DSSC	Dye Sensitize Solar Cell
DC	Direct Current
DI	De-Ionized Water
E. Coli	Escherichia Coli
EDX	Energy-Dispersive X-ray Spectroscopy
FE-SEM	Field Emission Scanning Electron Microscope
F	Fluoride
LB	Lysogeny Broth
M	Molarity
NaCl	Sodium Chloride
NH_4F	Ammonium Fluoride
NH42 SO4	Ammonium Sulfate
O	Oxygen
RO	Reverse Osmosis
Ti	Titanium
TiO_2	Titanium Dioxide

UV	Ultraviolet light
USNH	US national institute of health
V	Voltage
WHO	World Health Organization

Chapter1: Introduction

1.1 An overview on water treatment

World Health Organization (WHO/UNICEF) estimated that in 2012 one in nine people does not have access to a developed water source which is nearly 780 million people in the world [1]. Lack of clean water even in water-rich areas, highlights the importance of the researches on water treatment methods with the goal of lowering costs, energy consumption and the side-effects on environment [2]. Nanotechnology has improved the cost effective and eco-friendly water treatment processes, using nanoparticles such as nano-catalysts and metal nanoparticles, and nano-structured membranes as nanofilteration (NF) [3]. Nanotechnology is the science of studying and functionalizing materials at nanoscale (1-100nm) and aims to produce new nano-sized devices with novel properties by increasing the surface areas of materials compared to their bulk particles [4]. Increasing the surface to volume ratio will increase the sensitivities of the materials to physical, chemical or biological reactions.

1.2 Application of nanotechnology in water treatment

The technology is currently being used in water purification systems. In water filtration and purification as well as shipping industries, biofouling is unavoidable and can have significant economic impact. Biofouling is a heap of microorganisms attached to wetted

surfaces that can cause equipment malfunction [5]. It can also introduce a major health hazard. Nanotechnology has contributed coating techniques to inhibit biofouling [4].

Also nanofilteration membranes entitled to Loose RO (Reverse Osmosis membrane), are effective agents to purify water [6, 7]. Different types of membranes with various pore sizes are being used in drinking water production. Reverse Osmosis membranes with pore sizes less than 0.6nm produce pure water by applying 30-70 bar pressure. Nanotechnology offered nanofilteration with pore size in 0.6-5nm range running with 10-40 bar pressure to produce pure water with low molecular solutes [8].

Nanotechnology also suggests nanoparticles and nano-powders as effective biocide agents [2]. Nano-scale metal particles are active antibacterial against both gram negative and gram positive bacteria [2]. Metals such as Silver, Zinc, Gold and Copper are also being used as antimicrobial and antifouling materials. Their main drawback is that highly dispersed nanomaterials into water, should be separated before consumption [9]. Immobilization of antibacterial agent is a superior approach to solve this problem which is discussed in the following chapters.

1.3 Chapter organization

Chapter 2 gives a general overview on TiO_2 crystalline structures, a literature review of fabrication methods of TiO_2 nanotubes, and their application. Motivations and objective of thesis are brought at the end of the chapter.

Chapter 3 presents an overview on apparatus details of fabrication and characterization of the nanostructures.

Chapter 4 illustrates the fabrication of titanium oxide (TiO_2) nanotubes using anodization of a titanium (Ti) foil in an organic electrolyte. Details of the experiments and effects of anodizing variables on formation of TiO_2 tubes are presented.

Chapter 5 describes the procedure of silver deposition on the TiO_2 samples, and emphasizes on the importance of a reductive doping step before metal-deposition.

Chapter 6 provides an outline about antibacterial testing procedure of the fabricated samples.

Chapter 7 Conclusions and future works are brought in this chapter.

Chapter 2: Literature review

2.1 Aim of the chapter

This chapter presents a general overview on titanium oxide nanotubes productions, modifications and applications. Different techniques to fabricate Titania nanotubes (TiO_2) are described. How to optimize their photocatalytic properties and embedment of metal nanoparticles into their structures are demonstrated. Additionally some applications of Metal doped TiO_2 nanotubes are briefly described.

The final part of the chapter includes a discussion on objective and the motivation of this thesis.

2.2 Structures and properties of titanium dioxide

TiO_2 crystals exist in three different structures namely, Rutile, Anatase, and Brookite. They all contain a mixture of ionic and covalent bonding between Ti and O [10]. All three TiO_2 structures are illustrated in figure 2.1. Each of the octagons presents one TiO_6 and therefore, each Ti atom has six bonds with O and each O has three bonds with Ti atoms [11]. The most available natural structure is Rutile. Brookite structure tends to convert to Rutile which is the most stable structure at all temperatures [12].

The band gaps are 3, 3.2 and 3.11 eV for Rutile, Anatase and Brookite, respectively, and consequently TiO_2 is not a conductive material but it is wide band gap semiconductor.

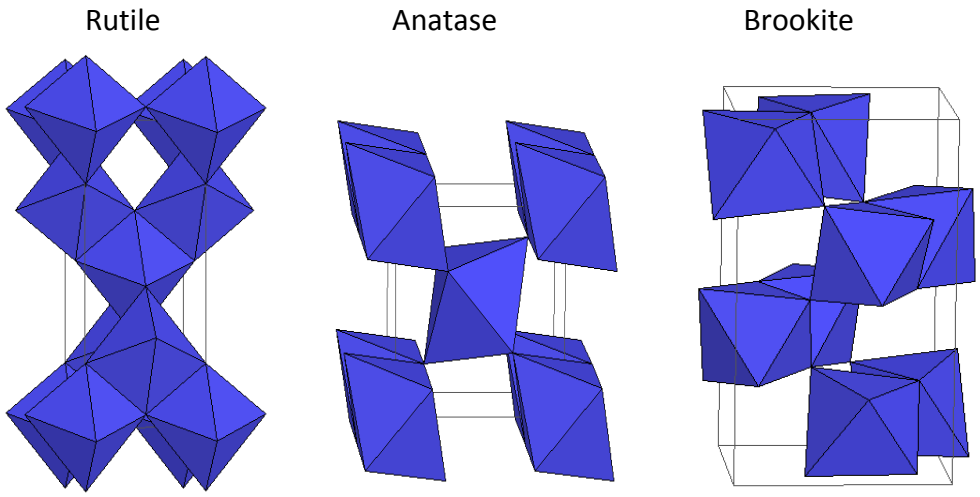

Figure 2.1. Various TiO_2 structures: Rutile and Anatase have tetragonal crystal structure and Brookite has an orthorhombic structure [11].

2.3 Fabrication of titanium oxide nanotubes

As it was mentioned before the physical, chemical, and biological sensitivity of materials increases as the ratio of surface to volume of the structures increases. For this reason, many structures/devices with the purpose of chemical and biological applications are fabricated in nanosacle sizes, like nanowries, nanotubes or nanoparticles. Accordingly, TiO_2 photocatalytic activity can be increased by maximizing its surface area; therefore various types of TiO_2 nanostructures have been synthesized. Among these nanosize morphologies, many research activities have common interests in nanotubes. Several fabrication techniques result in nanotubes with controllable diameter, length and wall thicknesses by adjusting the variable parameters.

In 1995 P.Hoyer reported the first production of TiO_2 nanotubes using an alumina template (AAO) [13]. The template is a porous alumina layer, grown on an aluminum foil substrate using anodization process.

Anodization is an oxidation process in which the metal is employed as anode in a two - electrode chemical cell. Self organized oxide nanotubes can be formed by metal anodizing in an appropriate electrolyte. In the case of Ti, use of fluoride based electrolytes results in formation of TiO_2 nanotubes. Fluoride ions dissolve titanium dioxide during the oxidation process, creating an array of free-standing TiO_2 nanotubes perpendicular to the titanium substrate [14-15].

Structure and morphology of the metal-oxide layer are strongly affected by the type of anodizing variables such as temperature, electrolyte, anodizing time and applied voltage.

The first generation of anodization process of titanium foils was reported in 1999 by Zwilling and co-workers. Their first study has shown different structures depending on various electrolyte compositions (CA, CA/HF) and metal substrates (Ti, Al and Ti/Al). They showed that fluoride ions in the electrolyte are absolutely needed to form the porous titanium oxide. The concentration of these ions in electrolytes affects the morphology of the oxide layer [16-17]. In fluoride-free electrolytes the oxide layer does not dissolve to form TiO_2 nanotubes but in presence of fluoride ions the formation and dissolution of the oxide layer occur simultaneously which lead to form TiO_2 nanotubes [15].

Latter works confirmed Zwilling findings and investigated other fluoride-base electrolytes in order to increase the length of the tubes.

J.M Macak et al. improved the tubes' length by tailoring the electrolyte's PH which is regarded as second generation process [18]. They demonstrated that at neutral PH the

tubes can be grown longer than 2µm. The tube length is limited in aqueous acidic electrolytes because they contain many ions which increase the electrolyte conductivity. Higher current results in fast etching and finally shorter tubes, but in neutral electrolytes the reduced chemical dissolution of TiO_2 layer leads to increase the thickness of the layer [18-21].

Third approach, optimizing tube lengths and sidewall morphology, was demonstrated in water-free organic electrolytes [22]. Although water accelerates the oxide formation, but it also increases the dissolution of oxide layer due to its conductivity [14]. In absence of water the low conductivity of organic electrolytes results in reducing the dissolution rate. In addition, viscosity of the organic electrolytes decelerates the ions transformation and the resulting tubes have more smooth walls than water base electrolytes; figure 2.2 [18, 20].

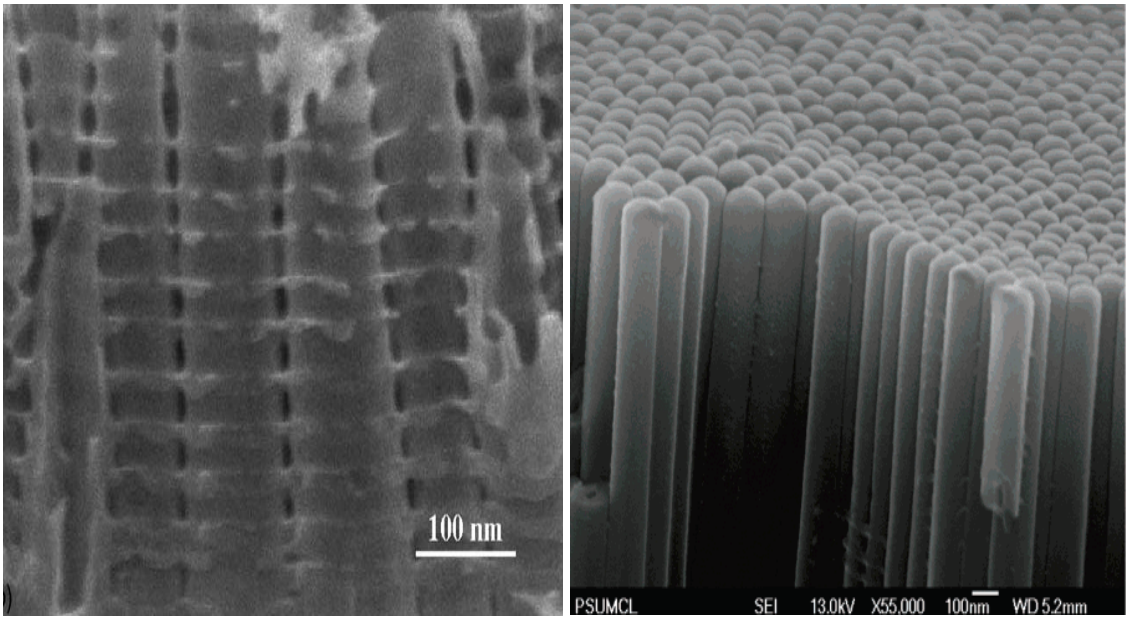

Figure 2.2. a) Sidewall ripples in presence of water [19], b)Smooth sidewalls in organic water free electrolytes [20]

The much slower anodization process in organic water-free electrolytes than water-based ones, results in forming a very smooth tube walls instead of having ripple structure.

The formation of anodized oxide layers are characterized by current-time curves. As it is illustrated in figure 2.3, the curves have three stages. At the first stage the current decreases in all fluoride contents then it remains at a steady state in fluoride-free and low fluoride cases and a compact oxide layer forms. In second stage the current increases for the fluoride base electrolytes and an irregular nano-pore layer forms. In last step the current drops again and a regular nanotube layer forms. The curves show that the current density increases as the fluoride amount increases in a range of 0-2% [14, 23].

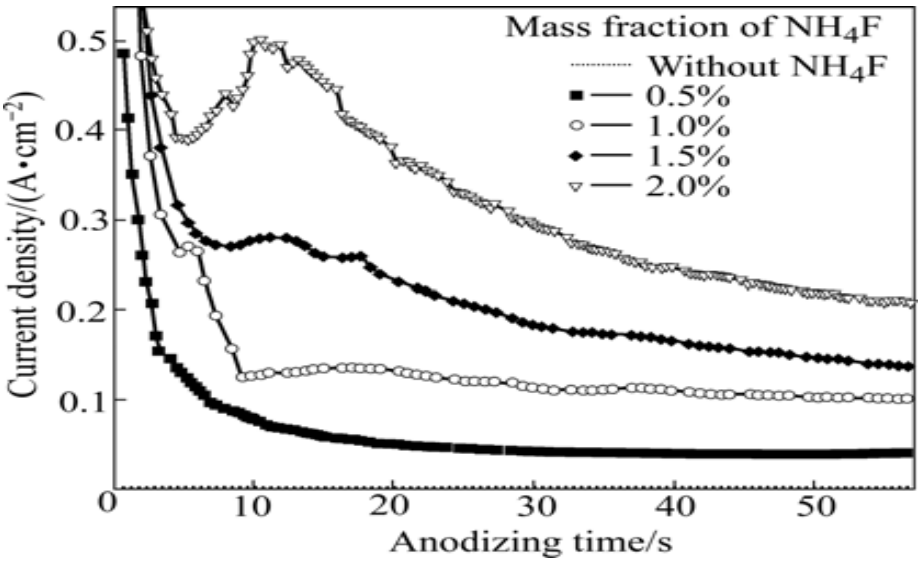

Figure 2.3. Current-time curves in various fluoride concentrations [23].

The effect of time, voltage and various electrolyte compositions on morphology of the oxide layer have been investigated in many works.

In the case of electrolyte, the dissolution and formation rate of the oxide layer are highly dependent on Fluoride concentration as well as PH and conductivity of the main solvent. The tube diameters are dependent on applied voltage. Higher voltages produce tubes with larger pores and thicker tube walls [16-17]. Choosing a constant current source leads to the tubes with various diameters due to the variation of voltage during the experiment [14]. Anodizing time controls the length of the tubes. Longer anodization time results in longer tubes [20, 24-26].

TiO_2 is a semiconductor with high photosensitivity and a large bandgap. However, the two main disadvantages of TiO_2 are its high electron-hole recombination rate and the lack of sensitivity to visible light. S.Sakthivel et al. showed that metal–doped TiO_2 systems can absorb visible light. Metal on TiO_2 surface also decreases the recombination rate because metal energy levels localize within TiO_2 bandgap and their valence electrons can be excited to the conduction band of TiO_2 with lower energies [27].

Due to importance of modified TiO_2, two metal-deposition methods are summarized as follow.

a) An approach to modify the tube walls is filling the tubes with metal nanoparticles. In the case of alumina template, deposition of metal into nanotubes can be directly performed by electroplating. In electroplating, metal ions in electrolyte solution coat the electrode or a conductive object in presence of electric field.

Yet electrodeposition fails for filling TiO_2 nanotubes, due to absorption of positively charged metal ions, the working electrode should be polarized with a negative voltage. Also it is known that TiO_2 is an n-type semiconductor with high resistivity, therefore, deposition starts from the top of nanotubes and blocks the tubes. Therefore, J.M.Macak *et al.* introduced a new filling strategy to overcome the problem [28]. By a self-doping process, they made the pore bottoms more conductive, while the pore walls stay extremely resistive. Positively charged metal ions in solution absorbed to the conductive bottom and filled the pores uniformly from bottom to top.

b) Silver nanoparticles could be deposited on titanium dioxide nanotubes by soaking the samples into AgNO3 solution followed by UV illumination to optimize the adhesion of silver and tubes or sputtering a thin film of metals followed by annealing the sample in 450˚C for 3 hours [29]. Figure 2.4 represents SEM images of silver Electroless deposition and gold sputtering doping.

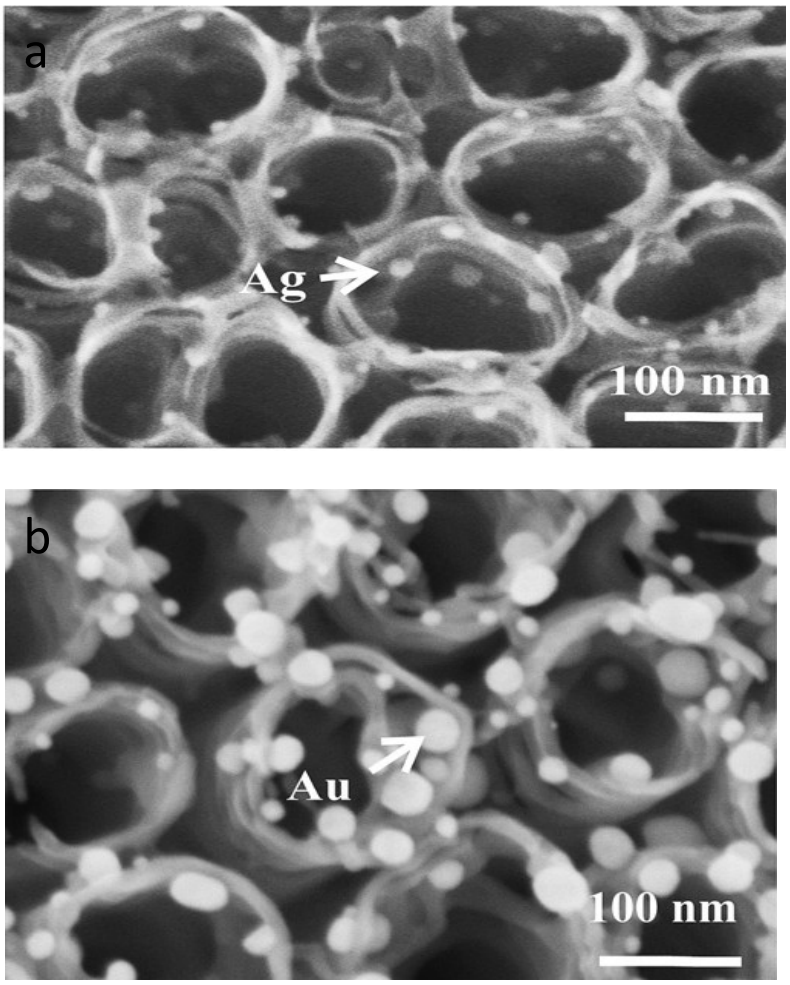

Figure 2.4. a) Ag doped TiO_2 nanotubes by soaking in AgNO3 solution followed by UV irradiation. b) Au doped by sputtering followed by annealing

2.4 Applications

TiO_2 nanotubes are being used in wide range of applications. Section 2.4.1 and 2.4.2 describe two applications in brief.

2.4.1 Antimicrobial effect

In water systems and equipment such as; shipping industries, ultra-filtration and water purification membranes, biofouling is unavoidable. Biofouling is a heap of microorganisms attached to surfaces, leading to equipment defects. Relating to microbes and the environment, different nanomaterials may inhibit biofouling [30]. TiO_2 is one of the most preferable materials for degradation of organic pollutants in water and water treatments due to its high stability, non toxicity, photo sensitivity and antimicrobial activity [27, 31]. This semiconductor is activated in presence of UV source, results in promotion of electrons from valence-band to conduction-band and leaving holes in valence-band. This positive hole in reaction with hydroxyl ions (OH^-) in water, produces hydroxyl radicals ($HO^\bullet$) which is more reactive than chlorine in disinfecting. TiO_2 modified surfaces presented antifouling behavior under UV light [30, 32]. To intensify the photocatalytic activity, the surface of the TiO_2 can be modified using metal doping. Metal nanoparticles, such as silver, have shown strong antimicrobial effect individually [33].

2.4.2 Solar cell

Classic dye-sensitized solar cells (DSSC) are based on TiO_2 nanoparticles. In DSSCs transparent titanium dioxide layer, with porous nano-structure, is coated with dye molecules. Dye molecules absorb light and produce excited electron-hole pairs which dissociate at dye-semiconductor interface. Electron migrates into the semiconductor and semiconductor acts like a path for the electron to the cathode. Oxidized dye molecules must re-charge from the electrolyte in a reduction process so the electrolyte provides electron for dye molecules from anode and acts like a path from anode to dye. Consequently there is a constant supplying electron at the cathode and constant receiving electron at the anode [34]. Figure 2.5 shows a schematic view of a DSSC cell.

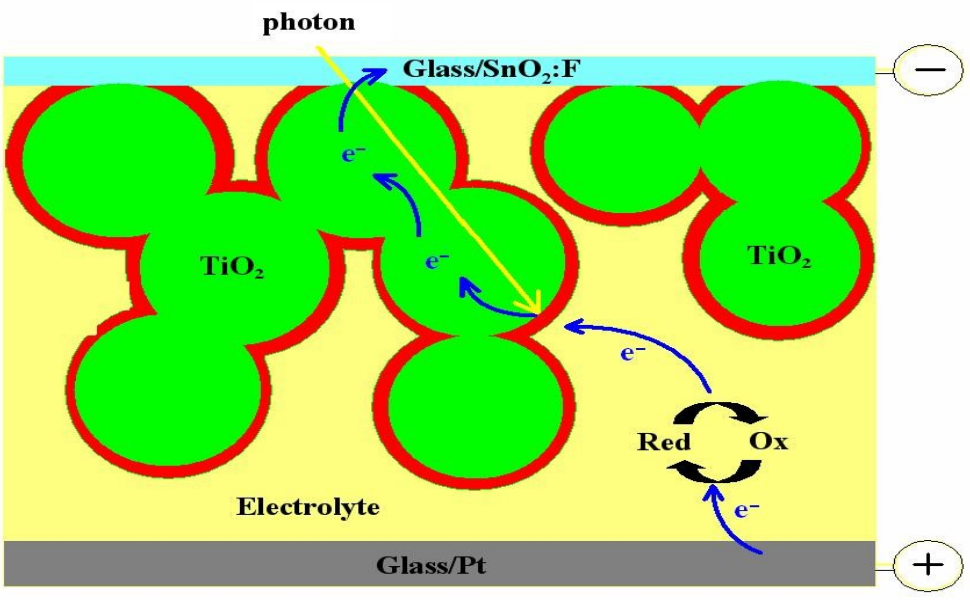

Figure 2.5. Schematic view of a DSSC. Excited electron of dye molecule goes to the cathode from TiO_2 lattice and oxidized dye recharges from anode by a Redox electrolyte [35].

In 2005 TiO_2 nanoparticles of classic DSSCs replaced with nanotubes for the first time, however in DSSCs, their use is not widespread [36].

2.5 Goal and motivation of the research

There have been several researches on the antimicrobial effect of titanium dioxide nanoparticles as well as novel metal nanoparticles in water disinfecting activities. Many of these works used various nanostructures such as nanoparticles to treat water. However, a main drawback with these methods is an issue to separate and remove the nanoparticles from the water after the treatment.

In this work we have studies the fabrication of TiO_2 nanotubes containing immobilized silver nanoparticles. To do this:

- Using electrochemical anodization technique TiO_2 nanotubes were fabricated. Having uniform and immobilized nanotubes attached to Ti substrate is the main advantages of this technique.
- Using electrochemical deposition we have embedded silver nanoparticles into TiO_2 nanotubes.
- Antibacterial activity of the samples was checked in Growth inhibition test against *E. coli.*

To the best of our knowledge, this is the first time that uniformly-deposited silver on a TiO2 array of nanotubes is fabricated and tested for antibacterial applications.

The partition of this thesis is based on four principles; fabrication of TiO_2 nanotubes, modification of their structures with metal nanoparticles, characterization of the samples, and finally their antimicrobial application.

Chapter 3: Characterization and measurement tools

3.1 Aim of the chapter

To determine the morphology of the fabricated samples scanning electron microscopy (SEM) is widely used in this research. In the case of resistive samples, sputtering device is being used to coat surface with a conductive material.

To find out the elements composing the produced samples, Energy-dispersive X-ray spectroscopy (EDX) was generally used. This chapter is allocated to describe apparatus details.

3.2 Scanning electron microscope (SEM)

Scanning Electron Microscopy (SEM) is one of the imaging devises which is broadly used in nanotechnology. This device provides images of the objects as small as 10nm using bombardment of the sample. As figure 3.1 indicates, a beam of highly energetic electrons is produced by the electron gun and passes vertically through the microscope, passing through the electromagnetic fields and lenses, irradiates to the sample as a concentrated beam. As soon as beam hits the sample, it excites electrons inside the sample and they will travel to sample surface. Several types of electrons irradiate from the sample surface such as Secondary electrons, backscattered electrons, X-rays and more (figure 3.2). Then, the detector collects the X-rays and primary and secondary electrons and converts them to signal which will be transferred to a display to produce

the final image. The brightness of any point of the image is influenced by the intensity of collected signals [37].

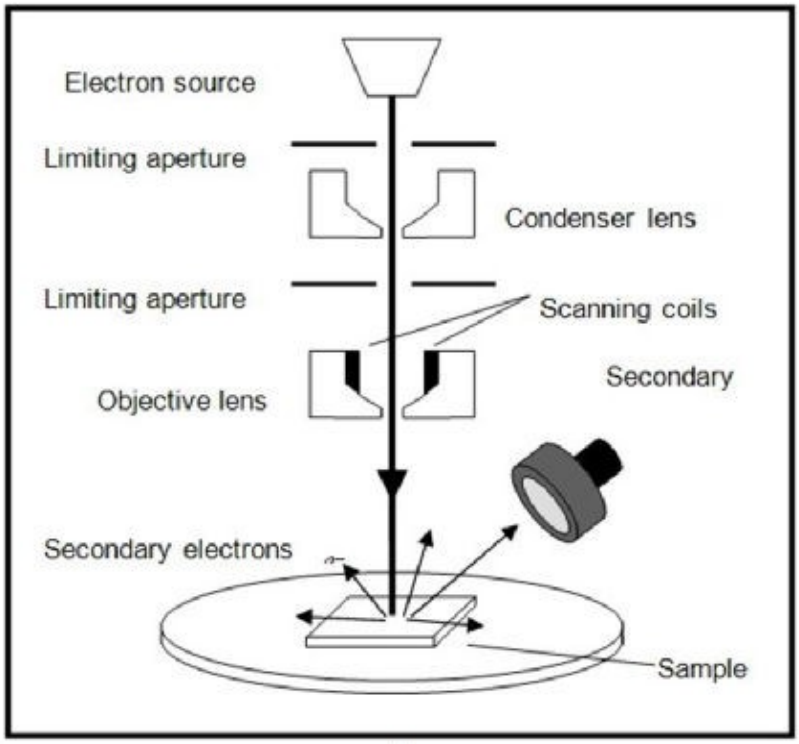

Figure 3.1. Electron beam passes through the microscope and hit the sample [38]

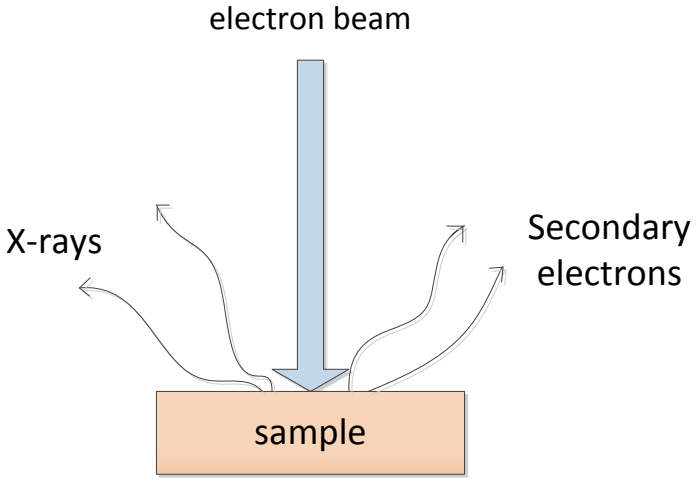

Figure 3.2. Secondary electrons are excited by primary electrons and move to sample surface. Afterward they will be collected to get a final image

In this work, an FE-SEM 4700 Hitachi has been utilized.

3.2.1 Sample preparation

To load the samples in the SEM chamber, they should be mounted on sample holder and then checked with sample height reference as shown in figure 3.3 to guarantee the appropriate height.

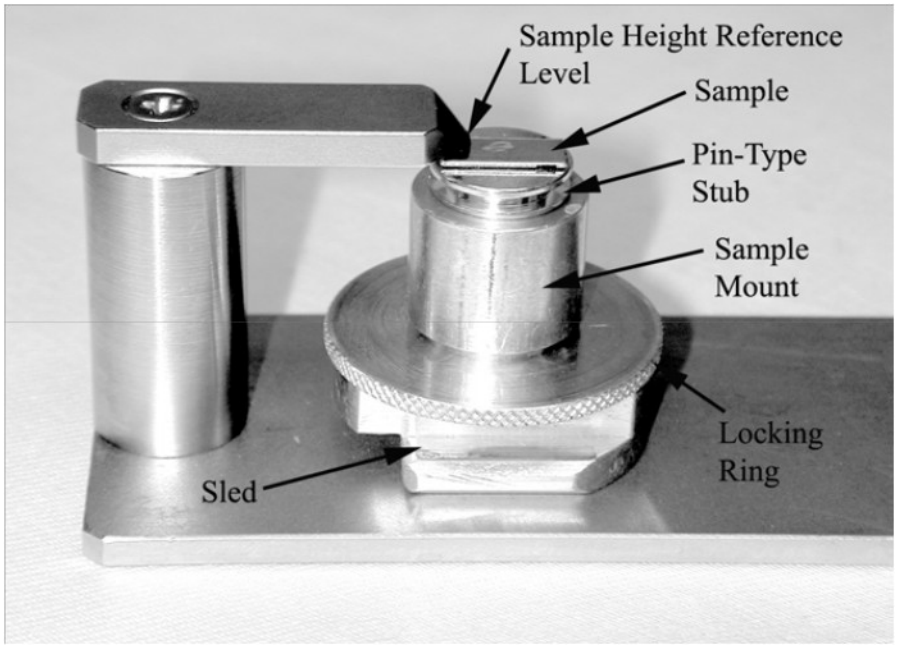

Figure 3.3. Sample height reference and sample holder [39]

After sample installation on holders, a non-conductive sample should be coated by a conductive element to increase the number of emitting surface electrons or should be partially covered by a conductive tape.

3.2.2 Sputtering

To coat a non-conductive sample with a few nanometers of conductive material we may use sputtering machine. This machine is an instrument for depositing a layer of target on substrate surface through the bombardment of the target with plasma. The process takes place in a vacuum chamber of a very low pressure argon gas. The gas ionizes with high voltage. Ions of plasma with sufficient energy bombard the target and provide free target atoms which travel to sample surface [40]. Figure 3.4 exhibits a schematic picture of the device.

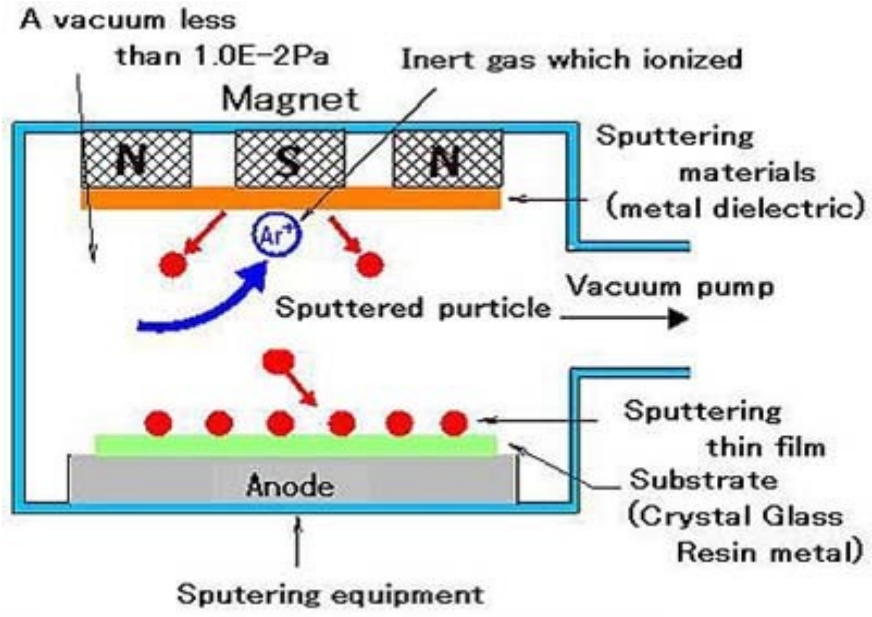

Figure 3.4. Sputtering Vacuum Deposition Process [41]

3.3 Energy-dispersive X-ray spectroscopy (EDX)

EDX or EDS is a device to determine the elements of specimens. To analyze the sample, it is bombarded by a focused electron beam. As figure 3.5, the applied electron beam excites the electrons in inner orbital of the atoms and removes it from the shell while leaving a hole in previous position of the electron. The electrons of the outer shell prefer to transfer to inner orbital with lower energy and fill the vacancy. The energy difference between the outer and inner shell releases as X-ray. A detector reveals the number and the energy of X-rays emitted from sample. As each atom has a unique atomic structure EDS can detect the elements. [42]

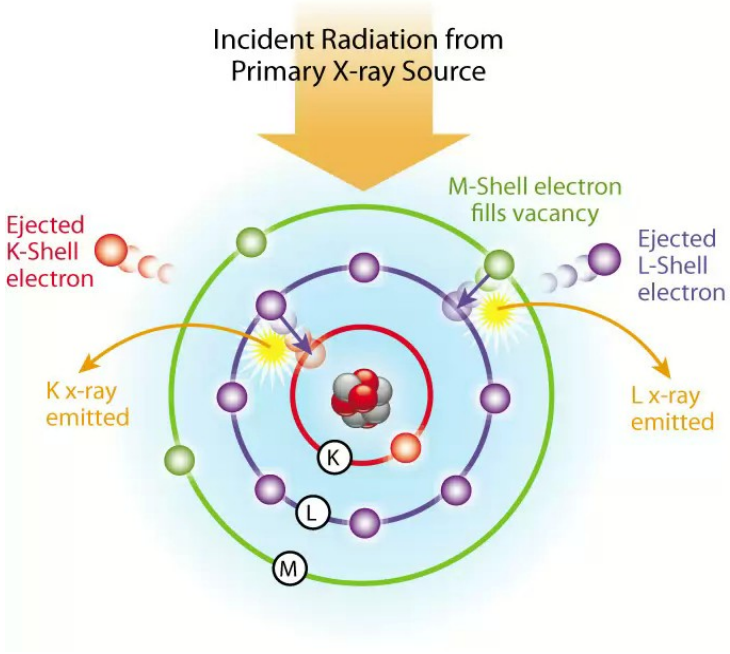

Figure 3.5. Principle of EDX [43]

Chapter 4: Titanium oxide nanotubes fabrication: results and discussions

4.1 Aim of the chapter

This chapter presents the fabrication of titanium oxide (TiO_2) nanotubes utilizing anodization of a titanium (Ti) foil. The effects of various anodization parameters like voltage, concentration of the electrolyte and the time of anodizing on TiO_2 nanotubes were investigated to optimize the tubes' structures.

4.2 Titanium anodization

Anodization is a process which results in forming an oxide layer on a metal surface. This oxidation is called anodizing process because the metal is placed as an anode in a two electrode electrochemical cell. The following sections demonstrate experimental set up and the effect of anodization variables such as; time, voltage and fluoride concentration in the electrolyte on nanotubes structures. The information of specimens' morphology was obtained by scanning electron microscopy (Hitachi S-4700 FE-SEM) in order to compare the length and the diameter of the tubes.

4.2.1 Ti foils initial treatment

High purity Ti foils (99.7%) with a thickness of 0.25mm purchased from Sigma Aldrich were cut 1cm×2cm samples. The samples were mechanically polished with sand paper

and degreased in three steps sonicating in acetone, methanol and DI water each for 5 minutes to achieve a mirror like surface. The samples then dried applying a nitrogen gun for 3 minutes immediately before anodization in order to avoid the formation of any native oxides.

4.2.2 Anodizing setup

Titanium anodization process, for preparation of TiO_2 nanotubes, includes an electrochemical cell with two electrodes, a DC power supply (Keithly 2400), an organic electrolyte and a magnet stirrer. The electrochemical cell contains a platinum plate as a counter electrode connected to negative voltage (cathode) and a Titanium foil as a working electrode connected to positive voltage (anode). A very slight stirring carried out to avoid local heating and facilitate the ions diffusion in the viscous electrolyte. All the experiments were done in an ambient temperature of 22˚C and the atmosphere pressure.

In all experiments the electrolyte consists of Ethylene Glycol Anhydrous 99.8% (Sigma-Aldrich), ammonium fluoride ACS reagent, ≥98.0% (Sigma-Aldrich) and Dionized water (DI) with different amounts of each, related to the objective of the experiments. As ethylene glycol is highly resistive a huge voltage drop occurs between two electrodes. Conductivity of the electrolyte increases by adding small amount of DI water and results in a quick formation of nanotubes.

The oxide layer started to grow once the positive voltage applied to the working electrode. The reaction at metal/oxide surface is:

$$Ti + 2H_2O \rightarrow TiO_2 + 2H_2$$

By applying a constant voltage, the current reduced continuously because metal particles were trapped by O_2 and formed oxide layer which behaves as an insulator, so it is a self-limiting process.

In electrolytes containing fluoride ions, the prepared oxide layer is porous because the fluoride ions react with the oxide layer and form the soluble $[TiF_6]^{-2.}$ So the oxide layer forms and dissolves at the same moment. The contest between forming and dissolving of the oxide layer, results in a self-organized TiO_2 nanotubes (Figure 4.1).

Dissolution of TiO_2 in presence of fluoride ions :

$$TiO_2 + 6F + 4H \rightarrow TiF_6 + H_2O$$
$$Ti^{4+} + 6F^- \rightarrow [TiF_6]^{2-}$$

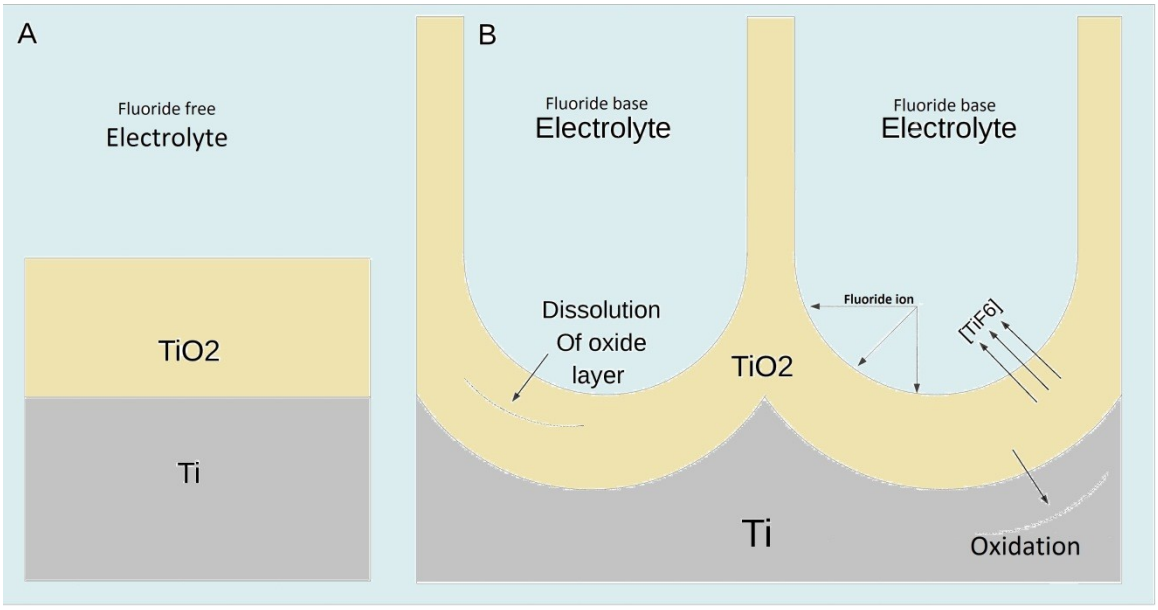

Figure 4.1. Anodization of Ti a) a compact oxide layer in absence of fluoride b) metal oxide nanotubes in presence of fluoride, oxidation of the metal and etching the oxide layer occur at the same time and results in formation of the tubes.

4.3 Characterizations of anodized samples

Most of the information about the oxide layer morphology was obtained by scanning electron microscopy (Hitachi S-4700 FE-SEM) and ImageJ tool developed by the US National Institute of Health (USNIH). SEM imaging was carried out in 5-10kV, with a working distance about 3-8 mm for top view and 5-8 mm for the tilted samples (in cross section view). Since TiO_2 nanotubes are not conductive, a conductive tape should partially cover the surface of the sample and the base, or a few nm layers of gold ions may be sputtered on it.

Excluding SEM information, Semiconductor Parameter Analyzer Keithly 4200-SCS and EDX also provided some information about the elemental analysis of the sample.

Semiconductor analyzer characterizes our device by presenting DC-IV plots. Figure 4.2 illustrates the graph resulted from Keithly 4200-SCS. It is consistent with the I-V plot of a typical schottky diode between metallic Ti and semiconductor TiO2. This will confirm the generation of semiconductor TiO2 nanotubes on the metallic Ti substrate. EDX spectrum shows containing material carefully in figure 4.3.

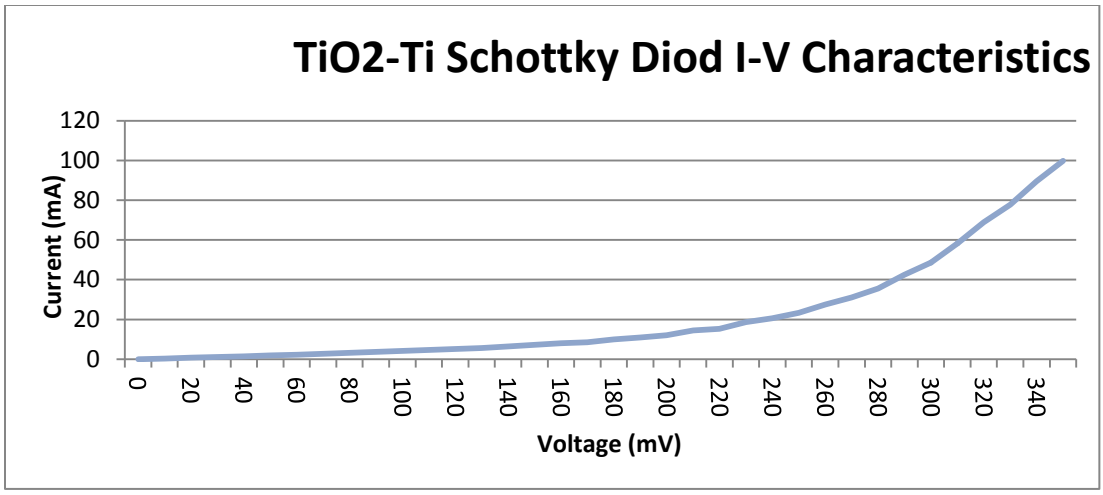

Figure 4.2. I-V characteristics of the specimens shows properties of the Schottky Diode

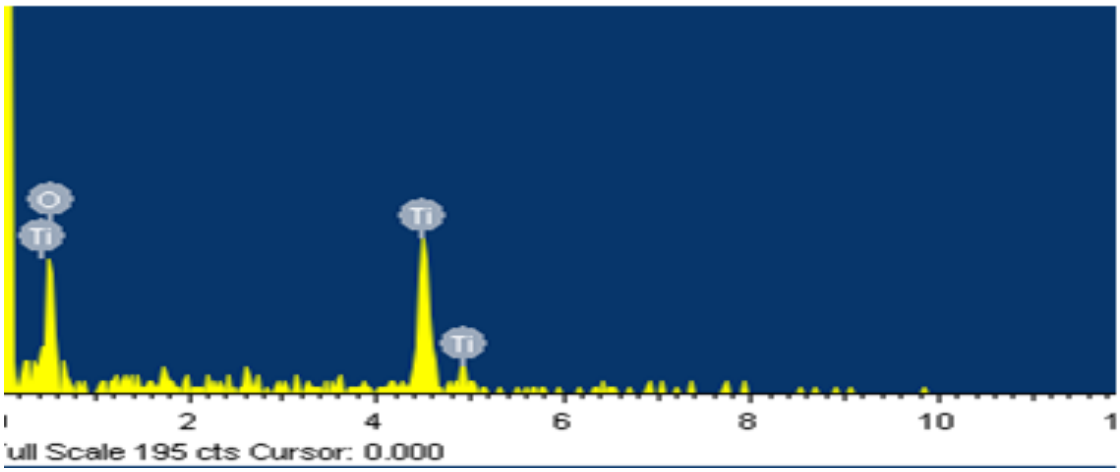

Figure 4.3. EDX analysis of the fabricated Ti-TiO_2 layer

In the following sections, the effects of anodizing variables on formation of TiO_2 tubes are presented in details.

4.3.1 The effect of fluoride concentration on formation of the tubes

Depending on the amount of fluoride ions in the electrolyte, the resulting structure is either compact or porous. In a very low fluoride concentration, the dissolution of the oxide layer is not enough to generate pores and the resulting oxide layer would be compact and pore-free. In a very high concentration no oxide layer could be formed due to the high etching rate of metal ions and solving in the electrolyte. So no metal ions could be trapped by oxygen. To obtain a uniform and regular nanotubular structure, a tolerable fluoride concentration may be used to adjust the generation and dissolution of the oxide layer.

To present the influence of fluoride ion concentration on tube formation, three experiments were carried out with various molarities (M) of ammonium fluoride. Table 4.1 contains a summary of the experiment parameters.

experiment	Voltage (V)	Time (h)	electrolyte (M)*
A	40V	2	ethylene glycol: H_2O (90:10 wt %)+ 0M
B	40V	2	ethylene glycol: H_2O (90:10 wt %)+ 0.15M
C	40V	2	ethylene glycol: H_2O (90:10 wt %)+ 0.36M

Table 4.1. Summary of the experiments

* Molarity (M) is a unit of concentration, $M = \frac{Number\ of\ moles}{Liter\ of\ solution}$

In all experiments, ammonium fluoride was added to water to dissolve homogeneously before mixing with ethylene glycol. Figure 4.4 shows that in fluoride-free electrolytes

the anodization results in a compact layer of metal-oxide. Small amount of fluoride ion is absolutely needed to form nanotubular morphology of the oxide layer.

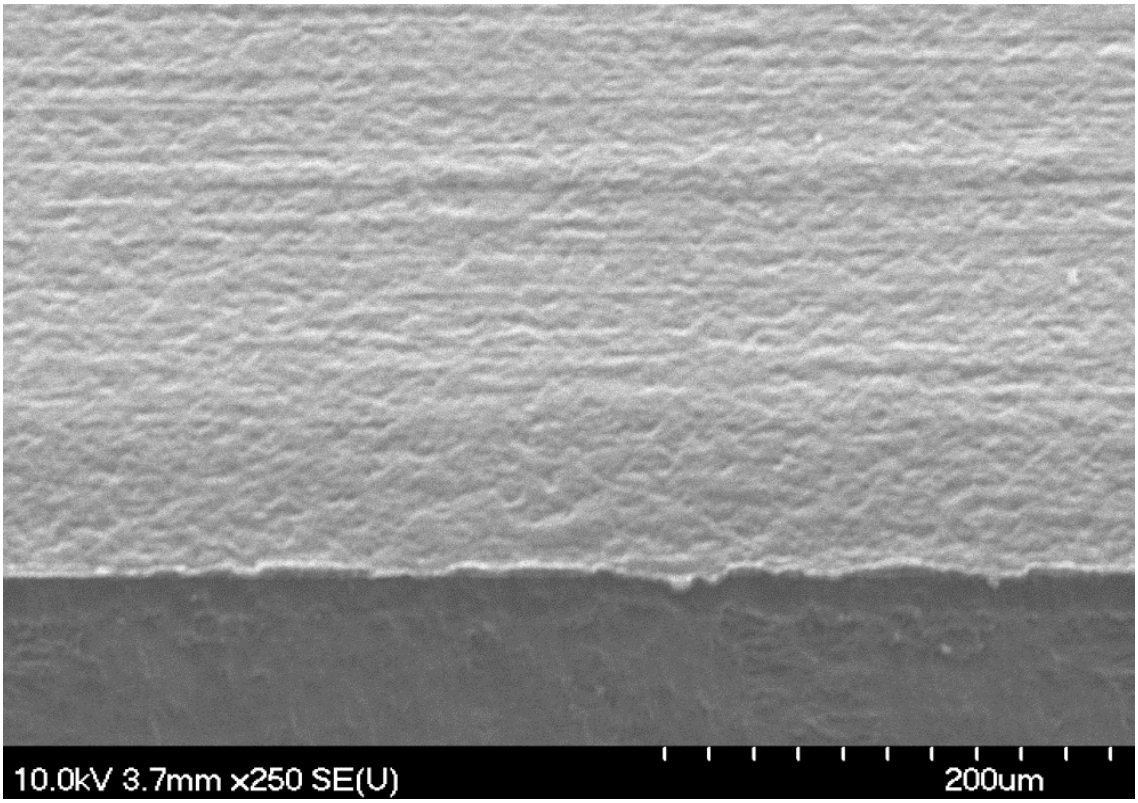

Figure 4.4. Formation of a compact oxide layer in absence of fluoride ions.

It was observed that using 0.15M and 0.36M ammonium fluoride promotes the porous structure and 2hrs anodizing gives rise to well-organized nanotube with equal diameters. But as illustrated in figure 4.5 electrolyte supported by 0.15M NH4F presented a better adjustment between oxidation and dissolution of the oxide layer while the one containing 0.36M NH_4F (figure 4.6) showed unwanted etching on top of the tubes and damaged tips of the tubes which collapse on each other.

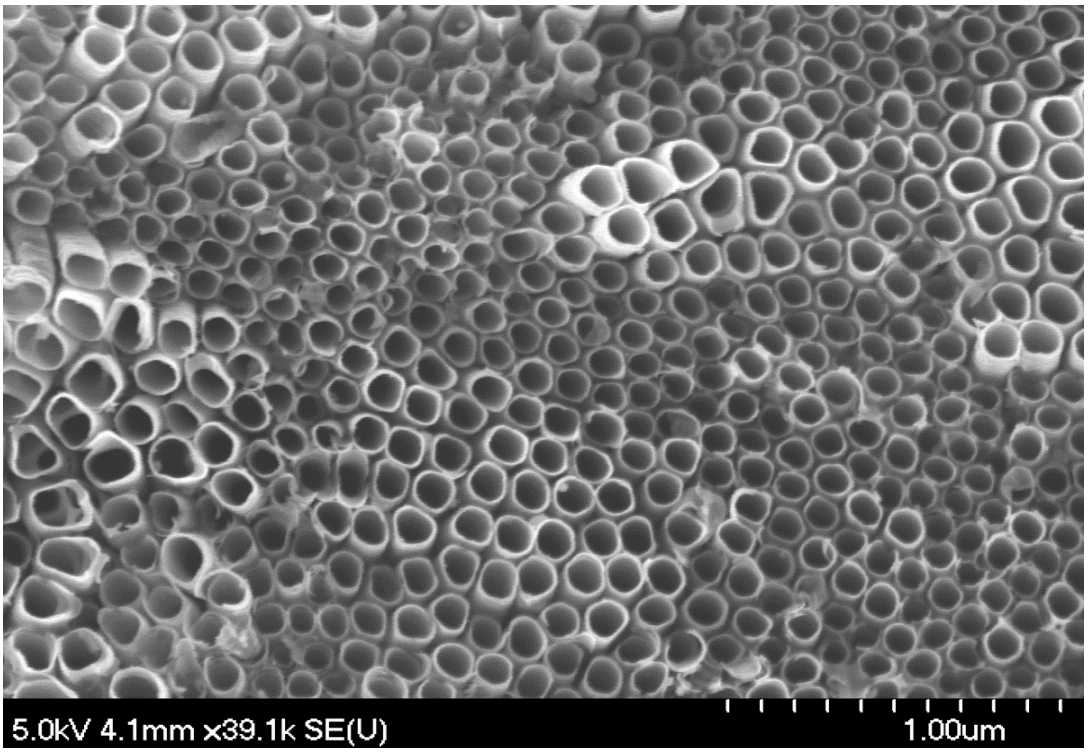

Figure 4.5. Anodization in presence of fluoride ion for 2hrs ,40V in ethylene glycol: H_2O (90:10 wt %)+ 0.15M NH4F

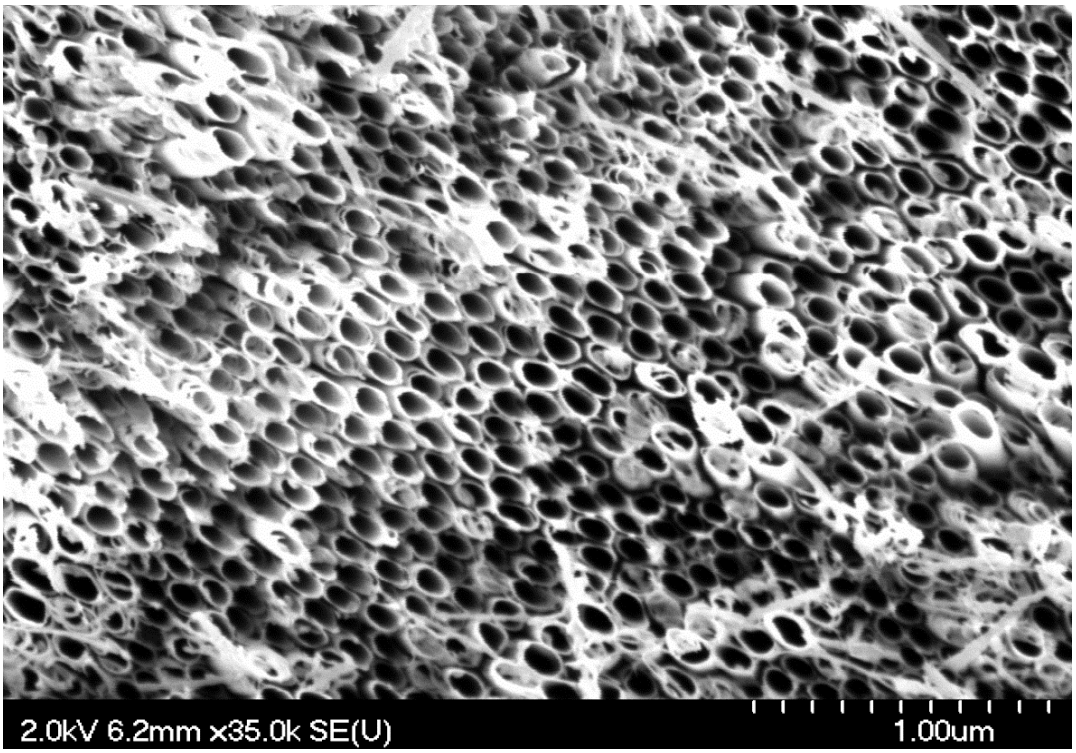

Figure 4.6. Anodization in presence of fluoride ion for 2hrs ,40V in ethylene glycol: H_2O (90:10 wt %)+ 0.36M NH_4F

4.3.2 The effect of anodization time on the tube structures

It was observed that the thickness of the oxide layer is mostly affected by anodization time. Nanotubes length increases in an extended time until an equality between oxidation and dissolution of the layer is obtained. After this moment, the length of the tubes remains independent from the anodization time. Generally shorter anodizing time results in more regular nanotubes. Nanotubes fabricated in longer anodization period are more bunched with some cracks. Since the dissolution occurs in the whole tube, longer anodization period results in less ordered nanotubes due to undesirable dissolving.

Figure 4.7 and 4.8 contains SEM images, showing the effect of time on obtained TiO_2 nanotubes using the same electrolyte solution. The electrolyte consisted of 0.36M NH_4F and ethylene glycol. Small amount of water (10%) was added to increase the conductivity of the electrolyte and therefore decreasing anodizing period. The experiments were performed under 40V for 2 and 4 hrs. Figure 4.7 confirms that shorter anodization time resulted in a uniform porous structure but as figure 4.8 shows by doubling the anodization period, increasing time, leads to cluster nanotubes which are blocked at the top by detached oxide particles. One must note that high fluoride concentration is also contributed to this undesirable structure.

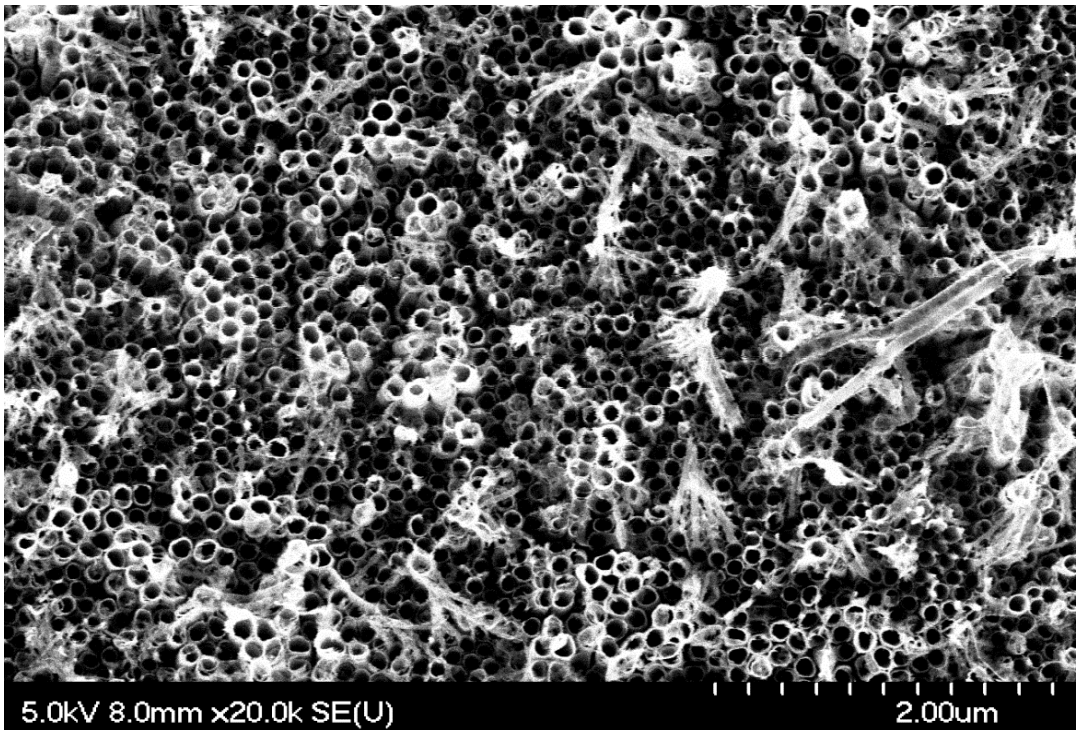

Figure 4.7. Anodizing in 0.36M NH_4F + ethylene glycol: H_2O (90:10 wt %) in 40V for 2hrs

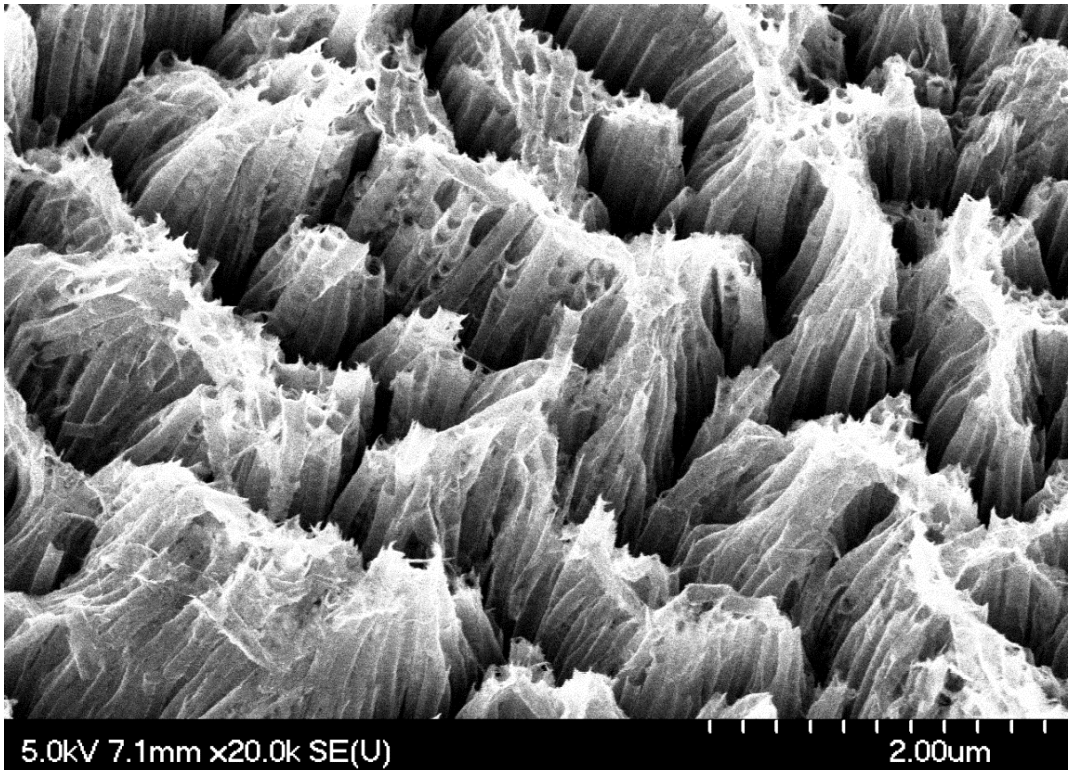

Figure 4.8. Cluster nanotubes generated as a result of increasing both the time and fluoride concentration.

To have a closer look on anodization time effects, we carry on two more experiments using lower fluoride concentration electrolyte and shorter anodizing time. Ethylene glycol: H_2O (90:10 wt %) + 0.15M NH_4F was prepared as electrolyte and the experiment executed in 40V for 1 and 2 hrs. In figures 4.9 and 4.10, SEM cross sectional images, clearly express the effect of time on thickness of the oxide layer. Obviously the more the time extended, the longer tubes formed.

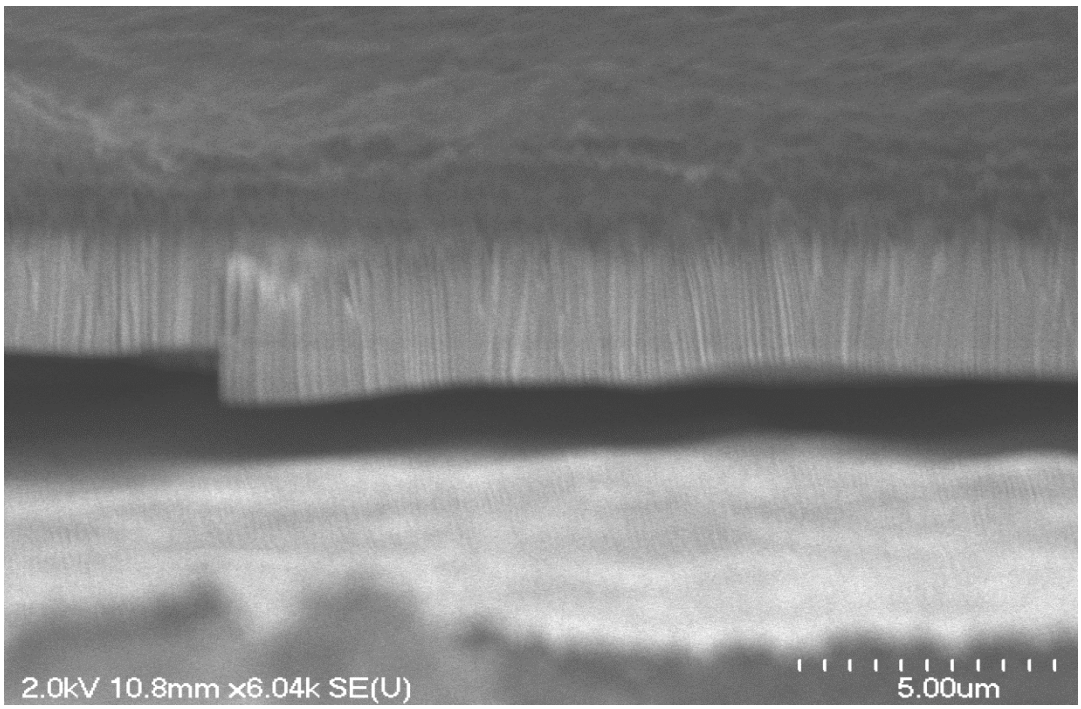

Figure 4.9. Cross sectional view of TiO_2 nanotube layer with approximately 2.78 µm length perpendicular to the substrate obtained from 2hrs anodization in ethylene glycol: H_2O (90:10 wt %)+ 0.15M NH_4F

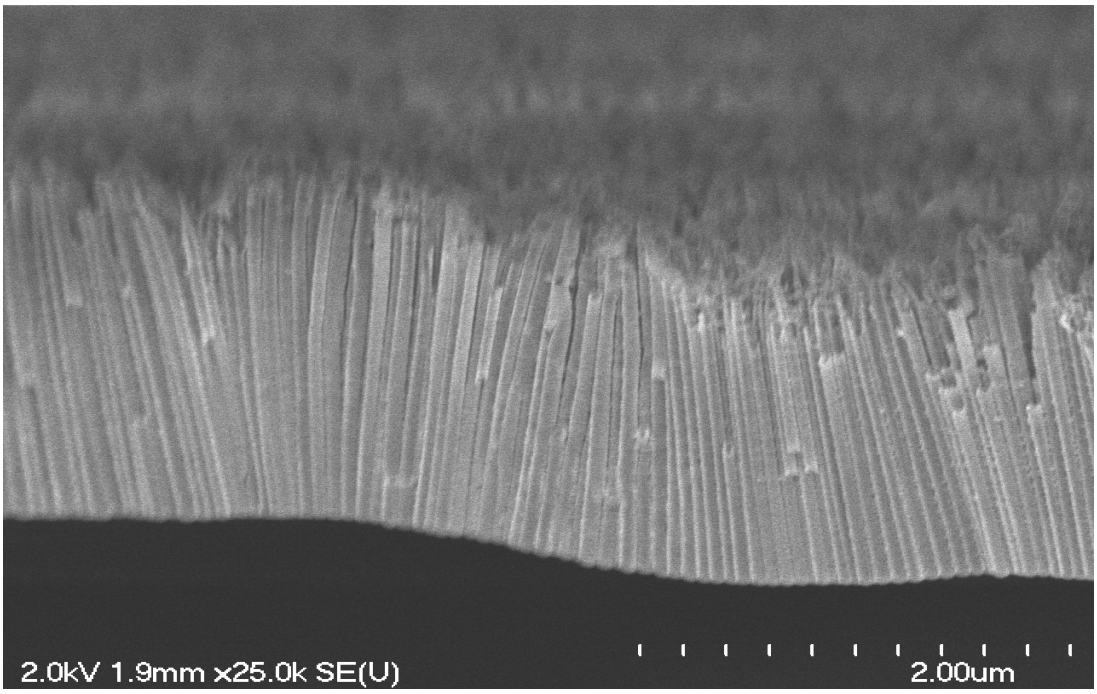

Figure 4.10. Cross sectional view of TiO_2 nanotube layer with at least 1.627µm length perpendicular to the substrate obtained from 1h anodization in ethylene glycol: H_2O (90:10 wt %)+ 0.15M NH_4F

4.3.3 The effect of voltage on diameter of the tubes

To find out the correlation between applied voltage and diameter of the tubes, anodization process was performed in an organic electrolyte for 2hrs under applied voltages ranging from 30V to 50V. In this study the electrolyte was prepared with 0.15M NH4F in ethylene glycol: H_2O (90:10 wt %) solution, with half an hour stirring to obtain a homogeneous solution. Three experiments using three various voltages of 30V, 40V, and 50V were carried out to study the effect of applied voltages on formation of the nanotubes. SEM images of the nanotubes are shown in figure 4.11.

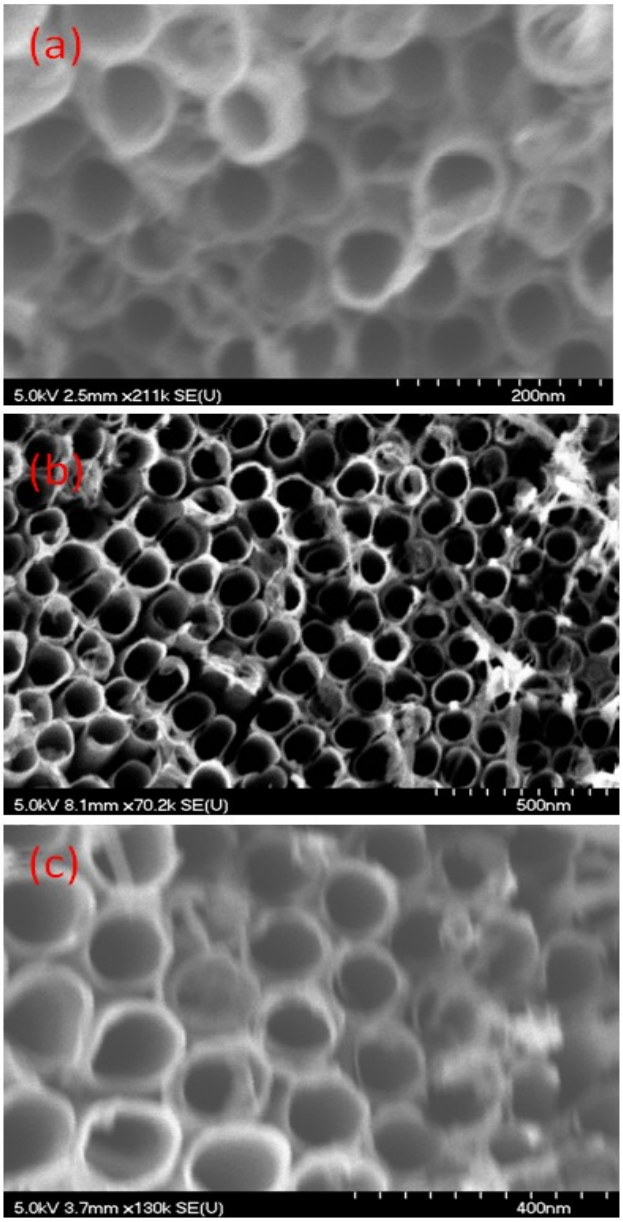

Figure 4.11. Effect of applied voltages on tube diameters of the nanotubes for 2hrs anodization time and in a electrolyte of 0.15M NH_4F + ethylene glycol: H_2O (90:10 wt %) at a) under 30V b) under 40V c) under 50V

As it is seen clearly, the higher anodization voltage resulted in larger tube diameter. Also tubes grown in higher voltages had thicker walls. Since the scales of these images are different table 4.2 indicates a summary of measurements calculated by ImageJ.

Voltage V	Tubes Mean Diameter nm	Tubes Min Diameter nm	Tubes Max Diameter nm	SD
30	58.633	48.607	67.348	6.008
40	90.424	82.839	98.206	5.629
50	118.536	98.514	141.004	11.58

Table 4.2. Effect of voltage on nanotube diameter -a summary of image measurements *(SD) standard deviation shows the variation of data from the average. Small SDs show that data are close to the mean value.

The augmentation of the diameters and wall thicknesses by increasing the applied voltage may be attributed to the current inside the electrolyte. Higher currents, as a result of higher voltages, produce thicker oxide layer.

Chapter 5: Silver Nanoparticles/TiO_2 fabrication

5.1 Aim of the chapter

This chapter presents the experimental procedures of deposition of silver nanoparticles onto TiO_2 nanotubes using three-electrode electrochemical cell in an appropriate plating bath under galvanostatistic current. Manipulation of TiO_2 nanotubes conductively using self-doping technique for the purpose of uniform deposition of silver nanoparticles are explained in detail.

5.2 Electrochemical metal deposition

Generally electrochemical deposition or electroplating is a process in which metal ions in electrolyte deposit on the electrode surface by applying electric filled or current. The fundamental principles to control Electroplating are current/voltage source, temperature, plating duration, electrolyte concentration, the distance between electrodes and stirring.

Among these factors, the source is an important task in optimization of deposition process. Since the electroplating manner is directly related to current, constant current sources are more preferred than voltage sources. Because when a constant current flows through the cell, the number of electrons determines the rate of deposition. Generally, applying constant currents result in a uniform deposition. The more the current increase, the faster deposition occurs. But using constant voltage results in fluctuations in current and as a result, uncontrollable deposition obtained [44].

5.2.1 Electrochemical deposition setup

Electrodeposition of metal into the porous titanium dioxide layer carried out in a three electrode chemical cell. As the cell is depicted in figure 5.1 the cathode is anodized TiO_2 on Ti foil, dipped into the electrolyte and connected to a galvanostat to supply constant current and a computer to record the potential between reference electrode and cathode. Counter electrode is platinum plate employed as an anode.

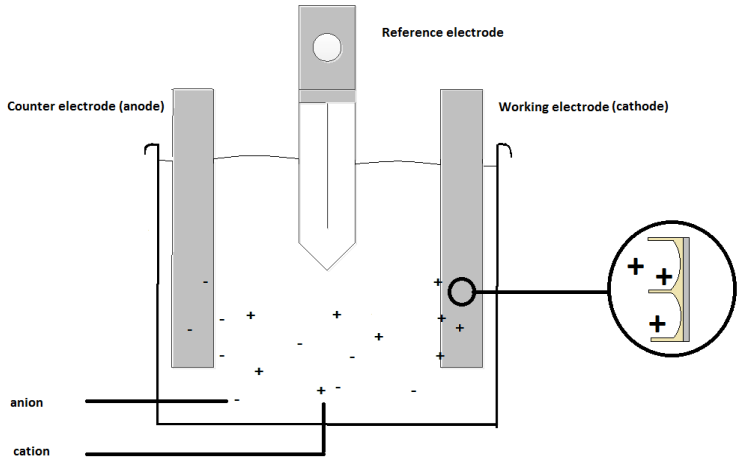

Figure 5.1. Schematic view of electrodeposition cell. As the cathode is negatively charged absorbs cations from the solution.

After setup preparation, electrodeposition performed in 1mA galvanostatic current in an appropriate solution, but a successful uniform metal electrodeposition was not obtained as illustrated in figure 5.2. This may be attributed to the high resistivity of semiconductor layer (TiO_2). Metal nanoparticles preferred to accumulate on previously deposited metal particles rather than on the more resistive TiO_2 layer.

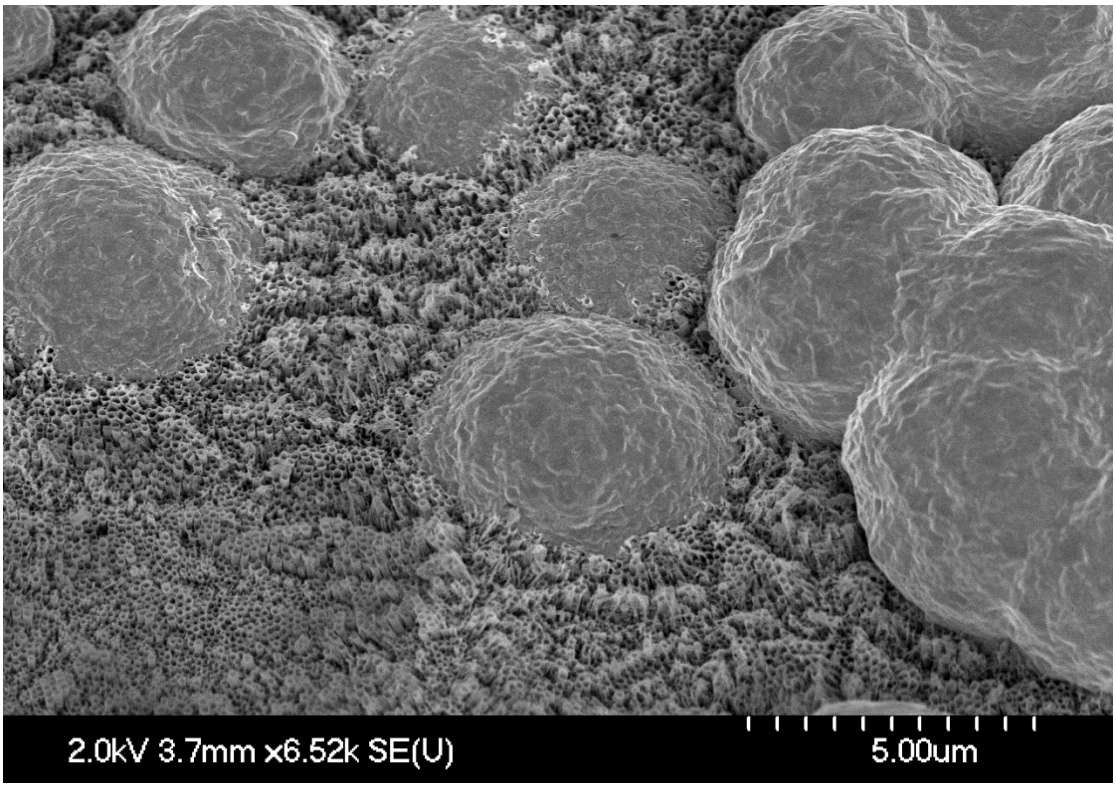

Figure 5.2. Aggregation of silver on top of the tubes due to high resistivity of nanotubes

During the process of the silver deposition, the Ti-TiO2 junction is reversely biased causing a large building potential (figure 5.3), between Ti and Ti oxide, making it a very resistive target and as a result, silver ions aggregate on top of the tubes rather than deposit inside the tubes.

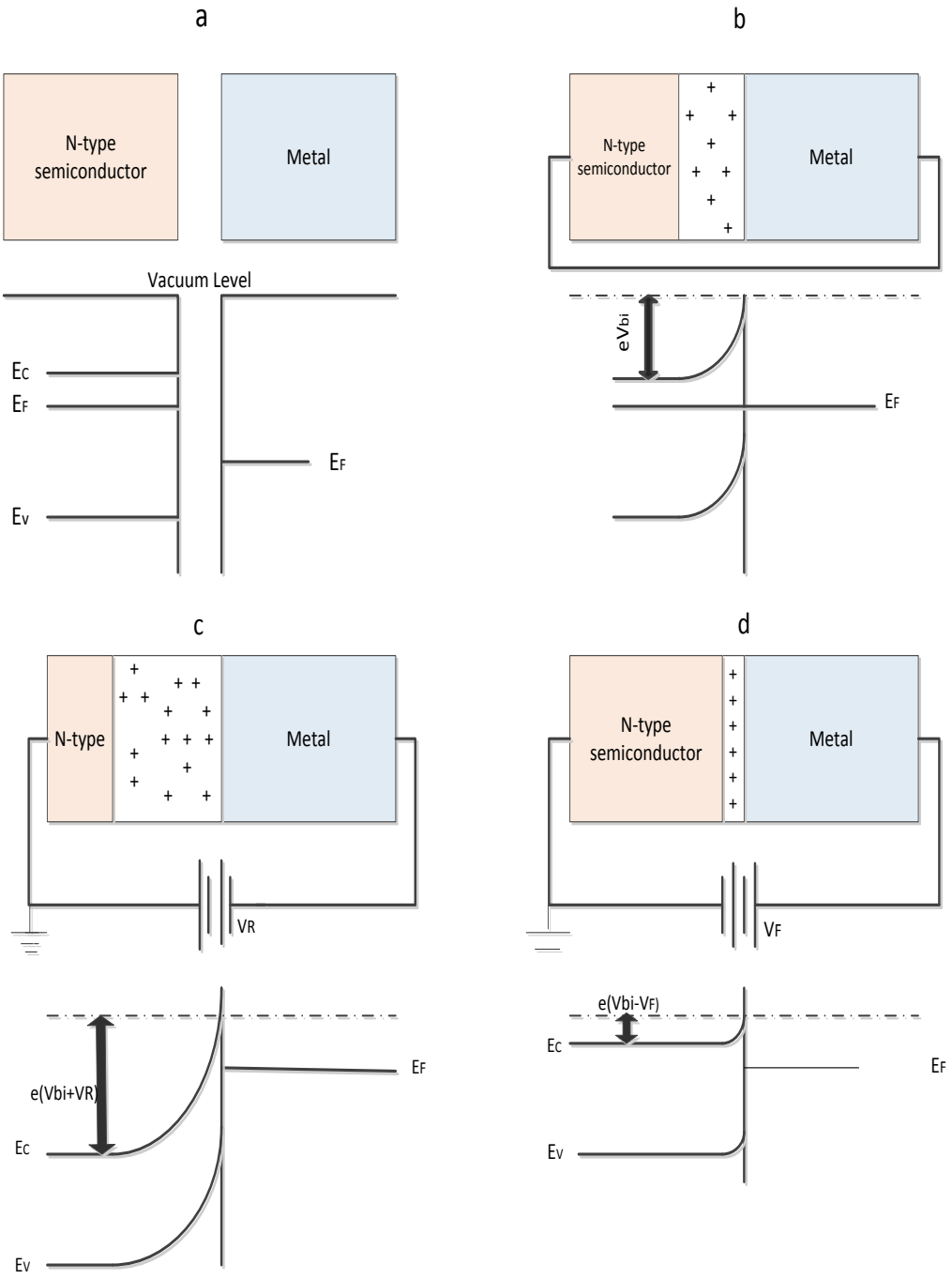

Figure 5.3. Metal-semiconductor energy-band diagram in different biases. a)separated metal and semiconductor band diagram. b) Depletion area generation by attaching them together resulting in Vbi. The energy band is bent in depletion area. c) metal-semiconductor in reverse bias and which properly justifies the huge resistivity of the oxide layer in reverse bias and d) metal semiconductor in forward bias [45].

In thermal equilibrium, as it can be seen in figure 5.3b, metal-semiconductor junction results in a single system with a single Fermi level. Electrons of semiconductor move into metal with lower energy level and create depletion region at semiconductor surface and build a potential which is exactly equal to the difference of the original metal and semiconductor Fermi levels. The potential that is called built-in potential.

Figures 5.3c and d compare the diode in reverse and forward biases. In forward bias the applied voltage decreases the barrier energy hence semiconductor electrons are able to move into the metal; as a result, semiconductor conductivity augments. In reverse bias the barrier level increases and semiconductor electrons cannot move through the junction [45-46].

5.3 Self –doping of nanotubes

In order to make TiO_2 nanotubes more conductive, $Ti^{4+}O_2^{2-}$ should be applied in a reductive doping process. In this process, the sample is negatively charged so it absorbs positive ions from the electrolyte and results in formation of Ti^{3+} which is more conductive than Ti^{4+}.

As TiO_2 is an n-type semiconductor with excess electrons and when TiO_2 electrons meet positively charged ions, the position of its Fermi level falls into lower energy. By decreasing the difference between metal and semiconductor Fermi levels, the barrier potential decreases and thus junction conductivity increases. Figure 5.3a shows the position of Fermi level while Øm>Øs. By adding H^+ into semiconductor, its Fermi level

moves down until Øm<Øs as figure 5.3a. In this case the junction is an ohmic contact which its energy band diagram is illustrated in figure 5.4b. In an ohmic contact if the negative potential is applied to semiconductor (figure 5.4c) the current passes easily through the junction and also when the negative potential is applied to metal (figure 5.4d) the electrons can move over the barrier because it is very small.

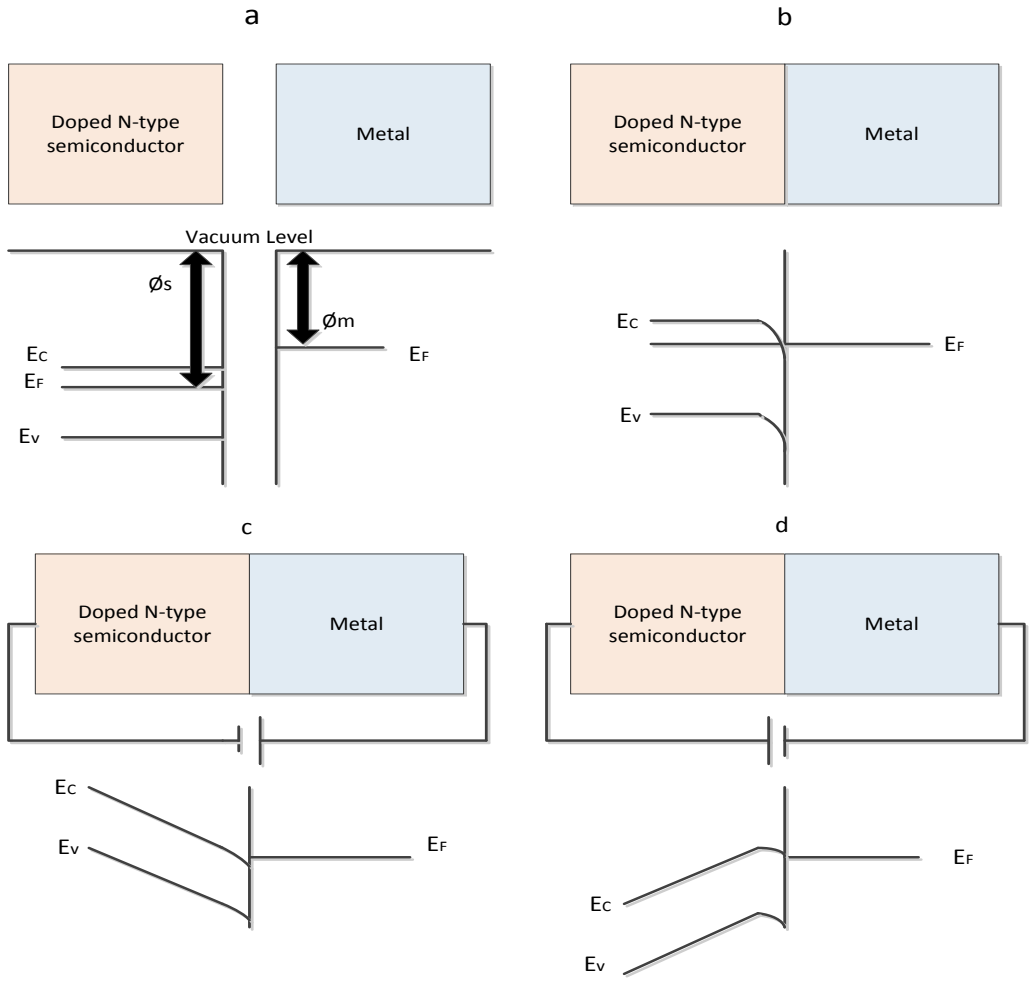

Figure 5.4 a) Doped-semiconductor and metal energy band diagram. b) Ohmic contact of metal- semiconductor due to Øm<Øs. c)Ohmic contact under forward bias d) Ohmic contact under reverse bias [45-46].

5.3.1 Experimental process of reductive doping

The reductive doping was performed in a three electrode chemical cell and the electrolyte was 1 M $(NH_4)_2SO_4$ solution. The working electrode was anodized TiO_2 nanotubes on Ti foil with more than 1μm length and about 100nm tube diameter, prepared in 1 hour anodization in 15M ammonium fluoride solution.

To determine the most appropriate reduction potential, cyclic voltammogram is a very effective tool.

This system includes a three electrode chemical cell, a potentiostat and a data recorder system. In this technique the voltage of working electrode varies between two potentials (A, B) with a certain sweep rate while current is measured. A plot illustrates current against applied potential. The current peak at a certain potential implies that, the reduction rate reaches to its maximum in that potential.

At the second potential (B), the potential switches negatively to make a distinction between oxidation and reduction processes.

Figure 5.5 illustrates the cyclic voltammogram between -2 to 0 V and vice versa with 500 mV/S sweep rate. As it can be clearly seen, in first half cycle, between A and B, the cathodic potential resulted in a reduction process which maximizes when the current peaks. At a cathodic potential around -0.8 V reduction reaches to its maximum rate.

In the second half cycle, from B to A, potential was scanned negatively to inspect the oxidation process in an anodic potential.

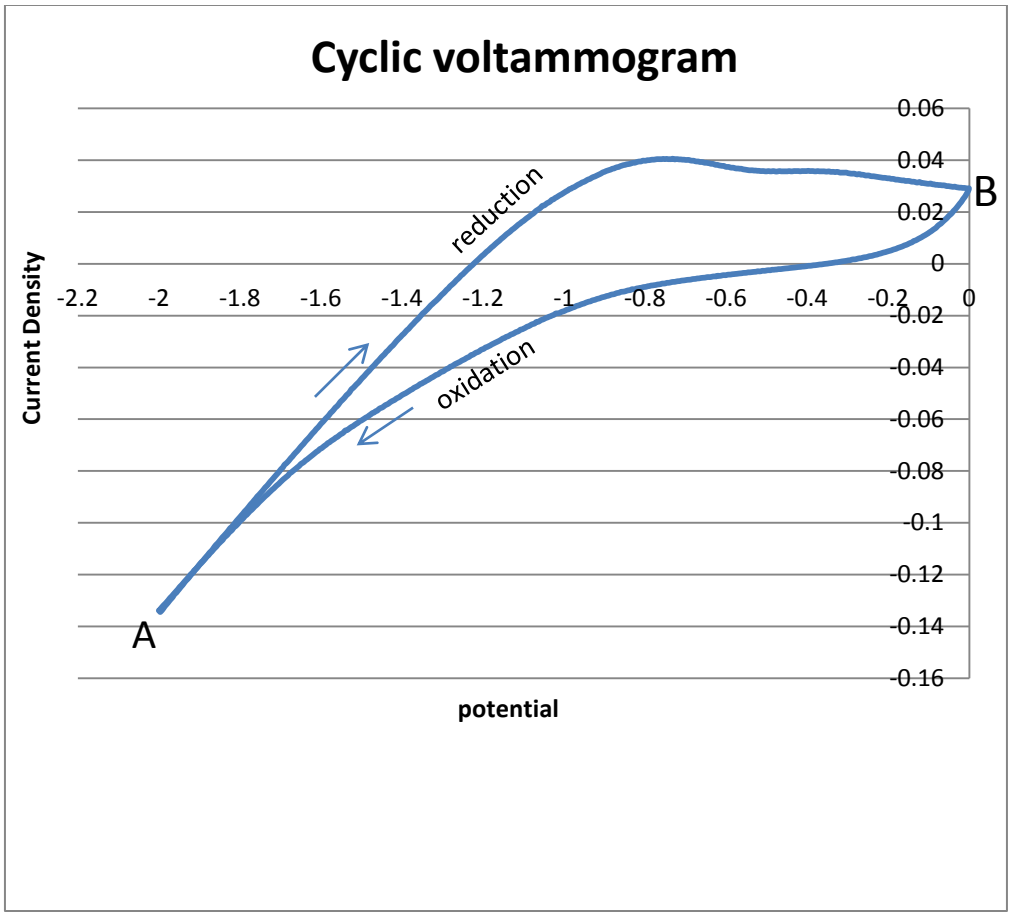

Figure 5.5. Cyclic voltammogram plot shows that -0.8V is a suitable potential for reduction of TiO_2 layer with nearly 600nm length.

Consequently, the samples were reductively doped in -0.8V cathodic potential in 1M $(NH_4)_2SO_4$ solution for a few seconds (2 to 6 seconds) before deposition process. Applying a longer time will damage the layer of the nanotubes. After only 6 seconds of reductive doping the resistance was changed from 358K Ω to 253 Ω. The reaction in working electrode is as bellow:

$$Ti4^{+}O_2^{2-}+e^{-}+H^{+}\rightarrow Ti3^{+}H^{+}O_2^{2-}$$

5.4 Metal deposition in TiO_2 nanotubes

Cyanide based silver solution (Silversene DW), purchased from TechnicInc company, was used for depositing silver nanoparticles in TiO_2 nanotubes.

The obtained TiO_2 nanotubes (described in previous chapter) with 1μm in length and 100nm in diameter were doped with -0.8V for only 6 seconds in 1M $(NH_4)_2SO_4$ solution thereafter the samples were rinsed and then sonicated in DI water to remove probable bubbles inside the tubes. The prepared samples were applied to electrodeposition cell with 1mA galvanostatic current for 20 minutes.

Figure 5.6 presents a comparison between metal deposition covering the tubes, before and after doping the samples. The difference is due to the conductivity of the working electrode (porous TiO2 layer). In figure 5.6b the DC current flows uniformly over the entire doped sample surface and results in a uniform silver deposition. On the contrary, in the case of resistive working electrode (un-doped sample, figure 5.6a), the non-uniform electric field between cathode and anode results in aggregation and non uniform deposition of silver nanoparticles.

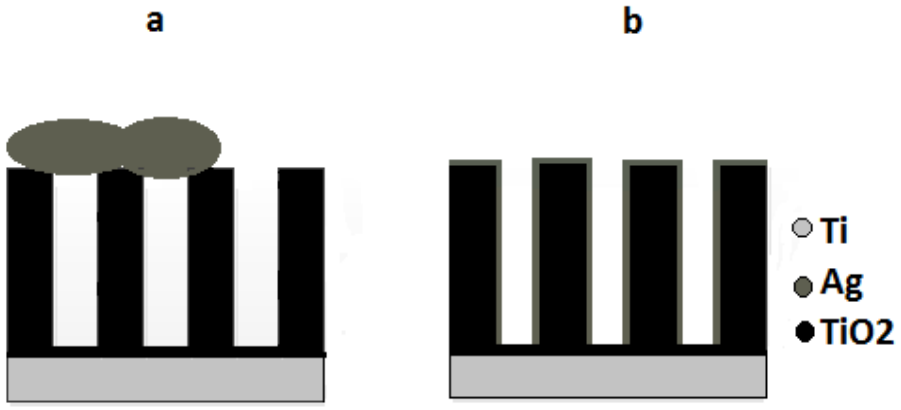

Figure 5.6. a) Metal deposition with constant galvanic current in resistive TiO_2 without reductive doping, resulted in blocking the tubes with metal aggregations b) Deposition at constant galvanic current after reductive doping process.

5.5 Characterization of the samples

The morphology of electrodeposited metal ions inside the nanotubes was determined by Scanning Electron Microscopy (FE-SEM, Hitachi S-4700). Samples were installed on the holder and were partially covered by conductive tape and placed into the chamber with 2KV and 10µA for voltage and current parameters respectively. Accumulation of silver ions on the tubes makes its surface uneven, so SEM images are not as clear as pure nanotubes. To analyze the elements and to make sure that the deposited materials are silver nanoparticles, elements spectrum and element mapping of Energy-dispersive X-ray spectroscopy (EDX) were used.

SEM images in figure 5.7 show that diffusion of silver nanoparticles improved by the doping procedure. The silver deposition on the TiO_2 layer may also be confirmed by the EDX analysis illustrated in figure 5.8. Additional F and C tags in figure 5.8 indicate the existence of small amounts of fluoride and carbon elements contained in the electrolyte

solution used in the earlier anodization stage. Figure 5.9 illustrates the distribution mapping of the silver element on the TiO_2 layer. It shows a uniform distribution indicating that the majority of the tubes are coated with silver.

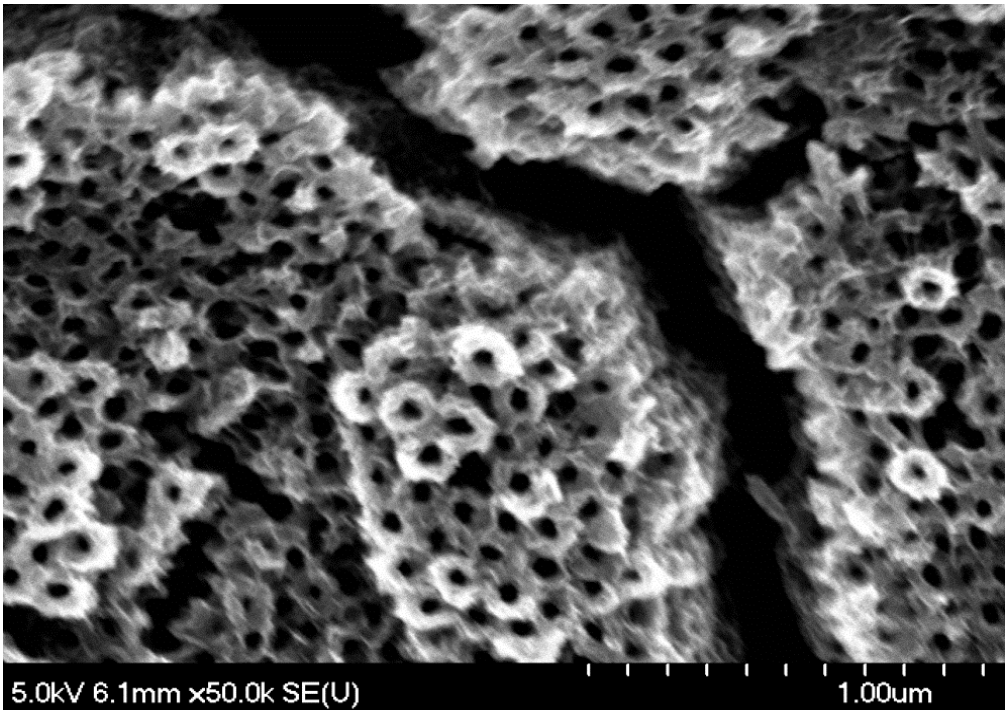

Figure 5.7. Silver deposited into the tubes after doping

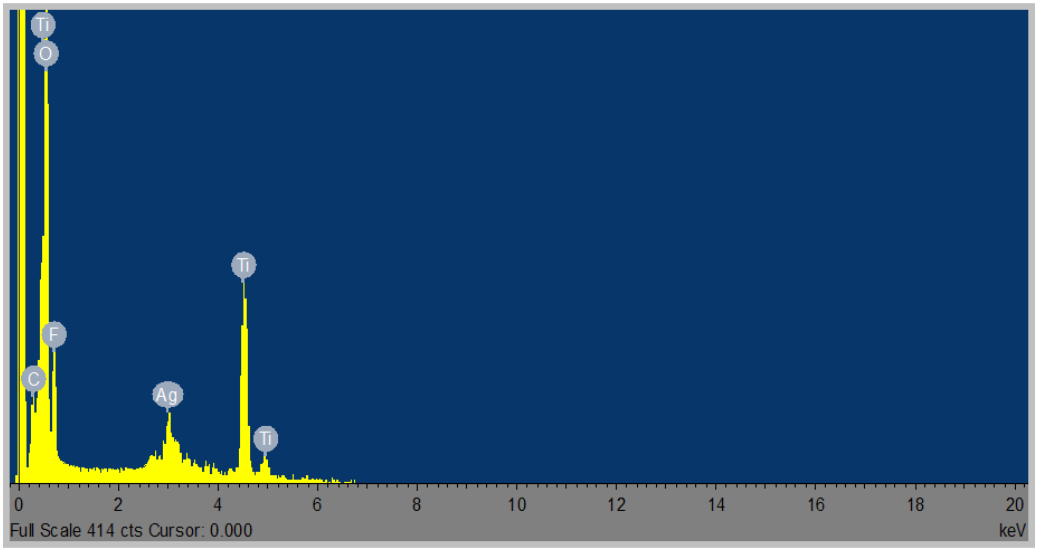

Figure 5.8. EDX elemental analysis

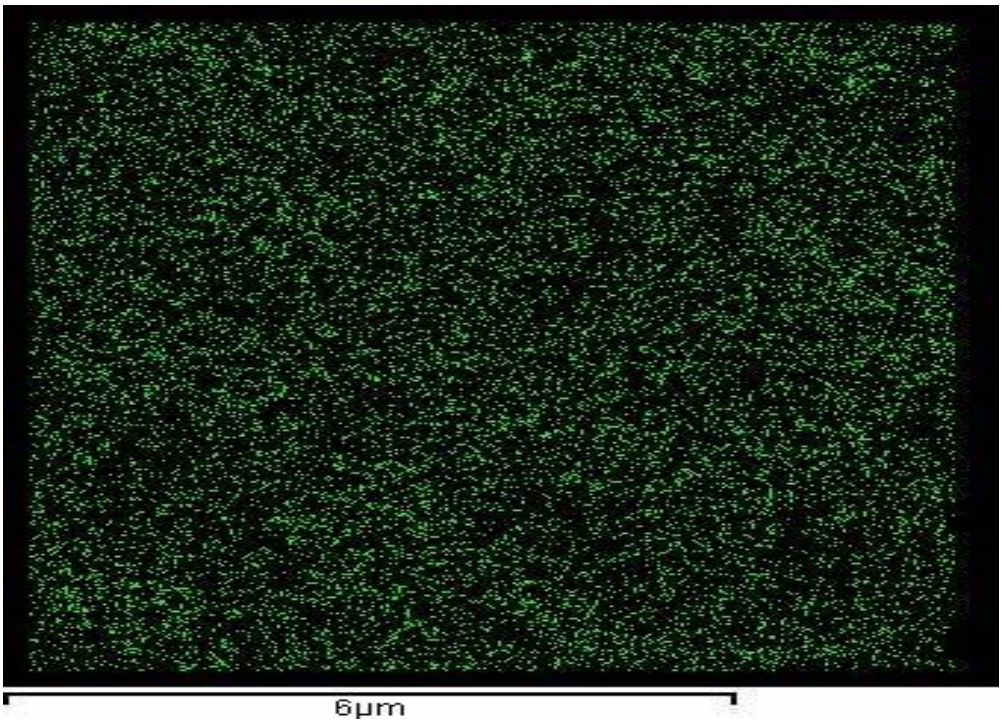

Figure 5.9. EDX elemental Mapping

Chapter 6: Antibacterial studies of silver modified TiO_2 nanotubes

6.1 Aim of the chapter

Both Silver and Titania nanoparticles are known as antibacterial agents, thus, their different nanostructures can be employed in water disinfecting applications.

This chapter will provide an outline about antibacterial testing procedure which is conducted on TiO_2 nanotubes and silver modified TiO_2 nanotubes explained in chapter 4 and 5. A Negative control (a sample free test) was carried out to compare bacterial growth in absence and presence of the nanomaterial inhibitors.

In all cases, growth inhibition test in Liquid Medium was selected to evaluate the antibacterial activity against Escherichia Coli bacteria, abbreviated as *E.Coli*. To verify the bactericidal effect of the samples, serial dilutions and plating were performed for counting the number of survived bacteria colonies.

To ensure that the results are reliable, the tests were triplicated with identical samples.

The following sections present the test method in details.

6.2 Escherichia Coli bacterium

XI1-Blue E. coli Strains grown in the Biological department of Concordia University were used as bacteria in this bacterium growth inhibition test. *E. coli* is a gram-negative and rod-shaped bacterium which lives generally in human and animal intestines. They are

mostly harmless but some of them can cause diseases or infections which can be transmitted to human body by contaminated water or food [47].

In the growth process of an *E. coli* bacterium, each cell divides into two cells. As all rod-shaped bacteria, once one cell becomes almost twice a regular cell it will break into two independent cells. The required time for *E. coli* duplication is nearly 20 minutes under the best culturing conditions [48].

6.2.1 Safety precautions for working with E.Coli

The experiment should be conducted in a laminar air flow table, equipped with flame sterilizer. Cultures must remain on the table at all times. Ethanol is used to disinfect the table before and after the experiment to avoid any contamination. All tubes and cells have to be labeled clearly and handled with gloves. All cultures and petri dishes must be disposed in biohazard bag and autoclaved before throwing away. Hands should be washed with soap before leaving the lab.

6.3 Methods and materials

Luria Broth, abbreviated as LB medium, is a standard solution for cultivation of *E. coli* which is composed of mineral, proteins, salts and ingredients that are needed to promote the growth of the bacteria [49]. Liquid and solid medium are prepared as follow:

To prepare 1 liter of the LB liquid medium 10gr Bacto-Tryptone, 5gr Bacto yeast Extract and 10gr NaCl were added to 950 ml of deionized water. To prepare the LB solid medium 15gr Agar was added to the composition as well. The composition was stirred until everything dissolves well and then the volume was adjusted to 1L. Then solution placed in autoclave for 50 minutes in 121˚C to sterilize before using (figure 6-1).

Figure 6.1. Well dissolved and clear LB solution after stirring

For this investigation an isolated colony of XL1-Blue *E. coli* Strains was inoculated with 2ml of liquid LB medium followed by shaking overnight in an incubator at 37˚C to culture enough bacteria for the test.

TiO_2 nanotube array and silver modified-TiO_2 nanotubes were tested as bacterium growth inhibitor. A control test was performed without nano-materials or any other

inhibitors as a reference test which is called Negative Control (NG). All tests were repeated three times to ensure their precision and accuracy. To have absolutely identical samples, a sample from a single experiment was cut into three equal parts with the size of 5×5mm.

To test the antibacterial efficiencies of the samples we have prepared three sets of culture tubes of Negative Control (NG), TiO_2, and Ag/TiO_2 materials. Each set contains three replications of the same material. So, all together we have prepared nine test tubes labeled as, A_1, A_2, A_3 (for the first set, NG), B_1, B_2, B_3 (for the second set TiO_2), and C_1, C_2, C_3 (for the third set, Ag/TiO_2).

All samples were exposed to UV light (λ=360 nm) for 10 minutes and placed into culture tubes containing 900 µL of liquid Luria Broth (LB). 100 µL of an overnight *E. coli* culture was added to each culture tube. Then, the samples were incubated on a rotary shaker at 37˚C at 250 RPM under visible light (35W lamp). After 6 hrs of incubation, the tube contents were diluted and labeled as A (1:10 dilution), B(1:100 dilution), C(1:1000 dilution), D(1:10000 dilution) and E(1:100000 dilution). The diluted samples were plated on petri dishes containing LB agar (solid LB) and incubated overnight at 37˚C. Individual colonies were counted to evaluate the bactericidal effect of TiO2 and Ag/TiO2.

Serial dilutions of the content of each culture tube were carried out as depicted in figure 6.2 to dilute the original culture in order to verify the number of viable bacteria, (the original culture is too condensed to count the number of bacteria).

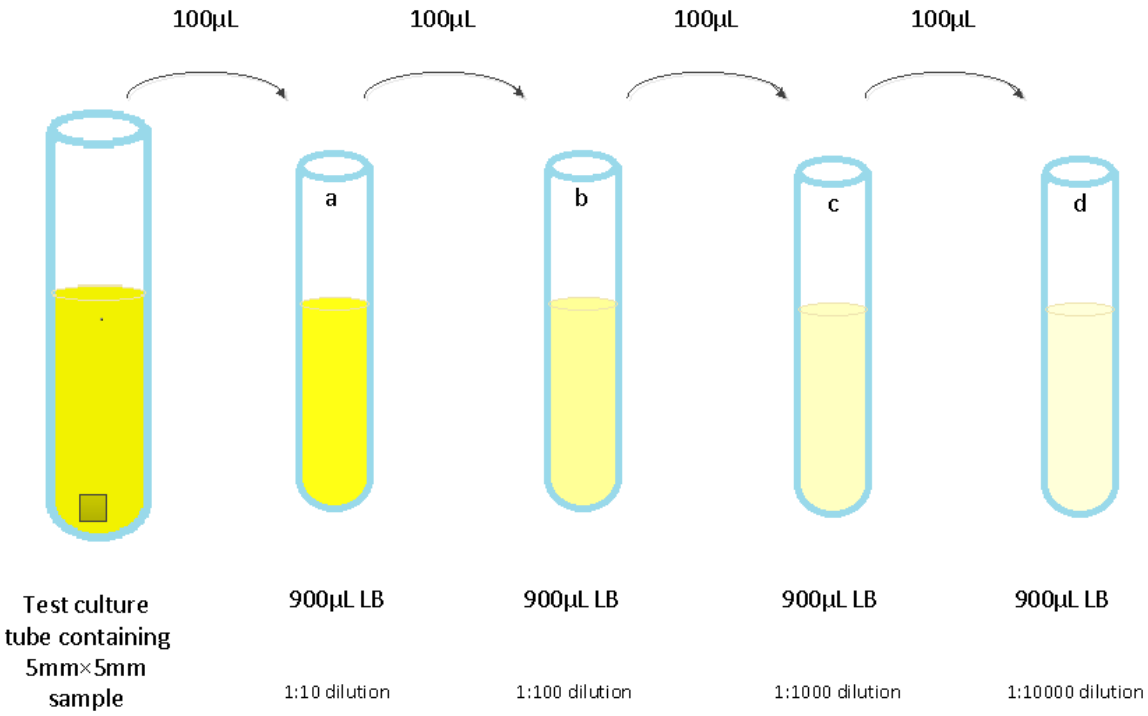

Figure 6.2. Serial dilutions was used to reduce the concentration of bacteria in the sample.

The diluted samples were plated on agar petri dishes containing LB agar and incubated overnight at 37˚C. Individual colonies were counted to evaluate the bactericidal effect of TiO2 and Ag/TiO2.

To prepare the agar petri dish the solid medium solution which has been explained earlier was purred in 100mm×15mm petri dishes as figure 6.3.

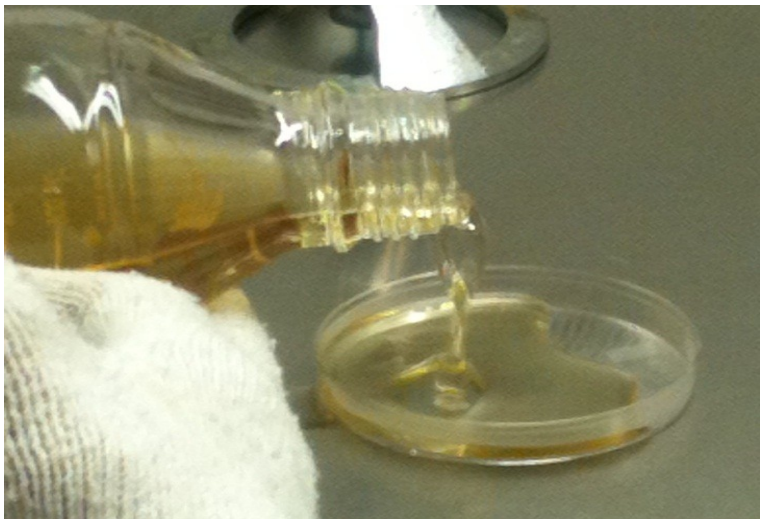

Figure 6.3. Preparing an agar petri dish

In the case of appearing bubbles on agar a flame passed by the petri dish for a moment in the same way as shown in figure 6.4 to remove them.

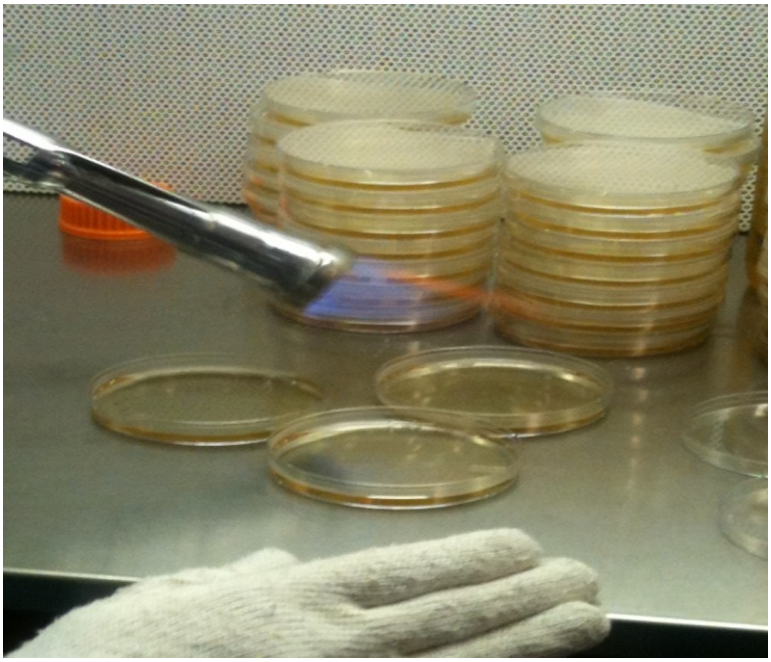

Figure 6.4. Removing bubbles from agar petri dishes by passing a fire flame over the dishes for a very short time.

Agar petri dishes should be prepared 24hrs earlier to solidify completely. Large number of petri dishes is needed to be ready before the experiment.

100µL of each dilution cell was deposited on the centre of an agar petri dish using a micropipette as shown in figure 6.5, and a sterilized "L" form glass rod was used to spread the bacterial culture on the agar surface. Then the petri dishes placed upside down in 37˚C heat chamber for 24hrs.

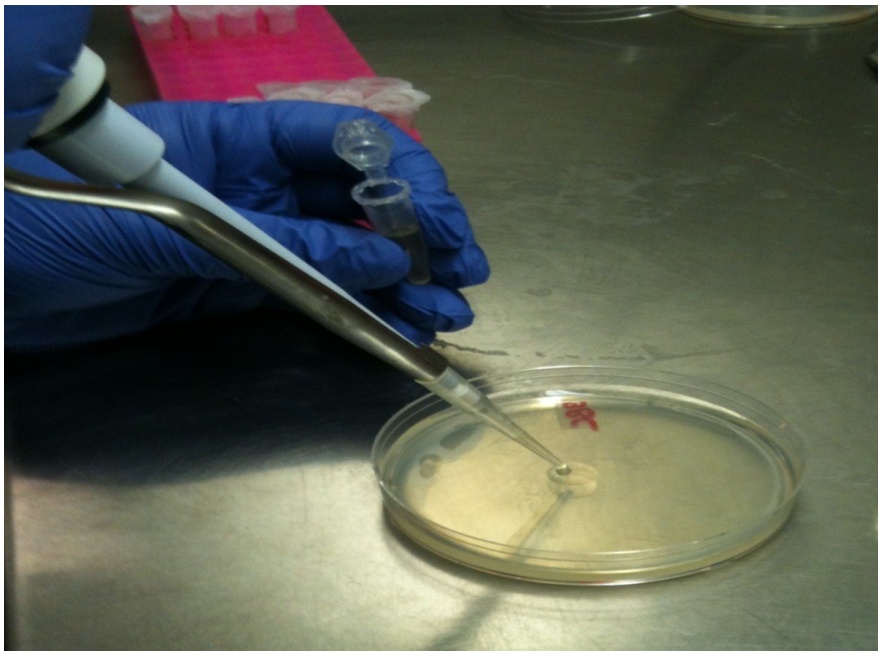

Figure 6. 5. Transferring diluted bacteria from dilution cell to agar plate by a pipette

To sterilize the rod, it was dipped into ethanol and passed through the flame. It should be used after cooling down because the hot rod would kill bacteria while spreading.

The length of incubation affects on the viable count. As a result of short incubations, the tiny colonies may be missed in counting since it has not had enough time to develop into its maximum size.

The following day the number of colonies was counted. Making a grid pattern on the petri dish is a helpful way to count the colonies correctly.

6.4 Results and discussions

The bactericidal activity of TiO2 and Ag/TiO2 samples against *E. coli* were tested in liquid medium test followed by serial dilutions and plating to measure the number of survived bacteria. In this test, TiO_2 sample was prepared in 1 hour anodization process using 0.15M ammonium fluoride electrolyte solution. Silver was electrodeposited on TiO_2 film for 20 minutes as it was explained in chapter 5. A Negative control (a sample free test) was carried out to compare bacterial growth in absence and presence of the nanomaterial inhibitors. The tests were conducted three times to show their reliability and repeatability. All diluted cells were plated however the first four dilutions (A-D dilutions) are too concentrated to count therefore the number colonies of the fifth dilution (E 1:100000) plates were counted, (figure 6.6).

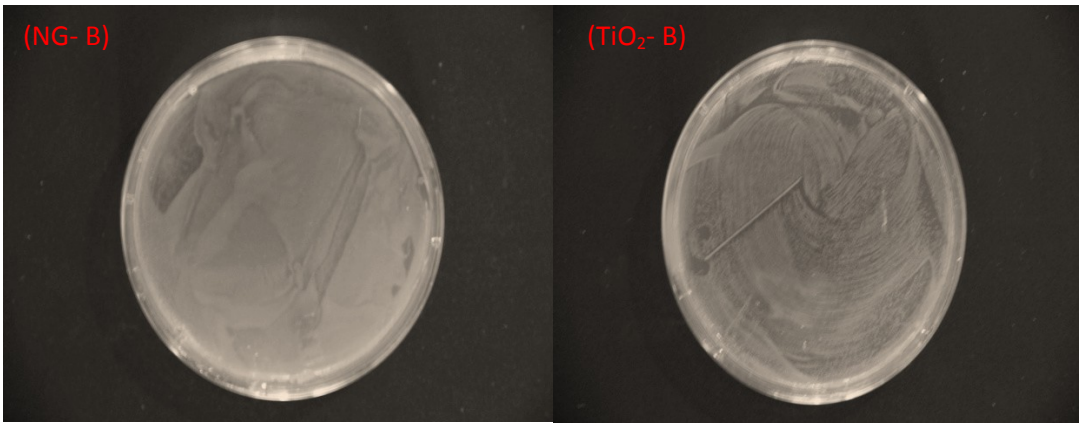

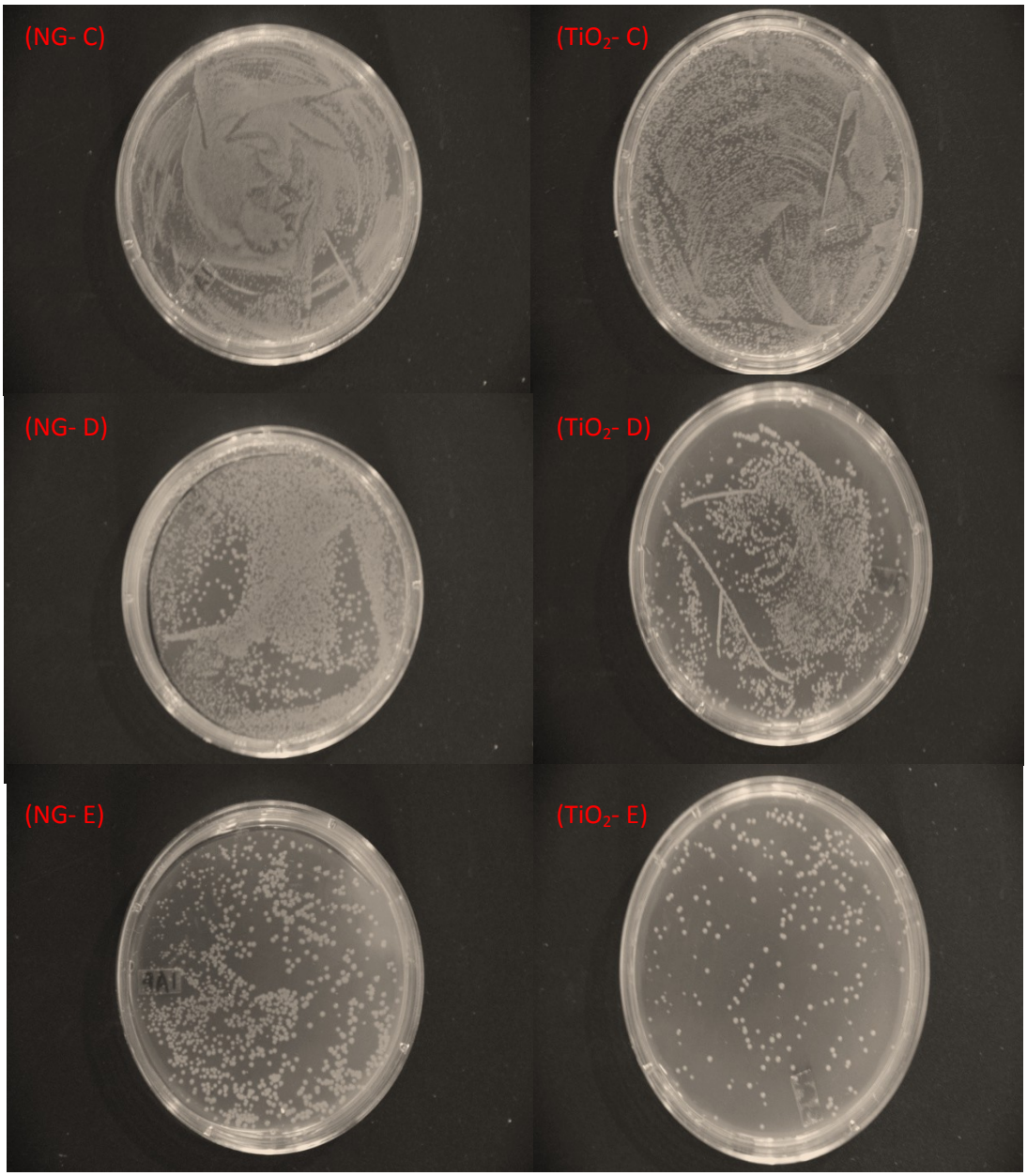

Figure 6.6. Comparison between serial dilution plates of the negative test and the tube containing TiO_2 sample. Left column shows negative test dilution plates (B, C, D and E respectively) and right column shows the test containing TiO2 dilution plates.

Figure 6.7 makes a comparison among the E dilutions of three tests, NG, TiO_2 and Ag/TiO_2, in 6 hour contact time, which confirms that TiO_2 sample showed a very powerful inhibition.

The quantity of the colonies decreased from 571 (±20) in Negative control to 228 (±12) using TiO2 sample which indicates approximately 60% inhibition efficiency.

Figure 6.7C shows no viable bacterium colony for sample E. when the cells were exposed to the Ag/TiO2 nanomaterial. The same results were obtained for all the Ag/TiO2 samples regardless of the dilutions that were tested. These results indicate that the Ag/TiO_2 nanomaterial is a very effective *E. coli* bactericide.

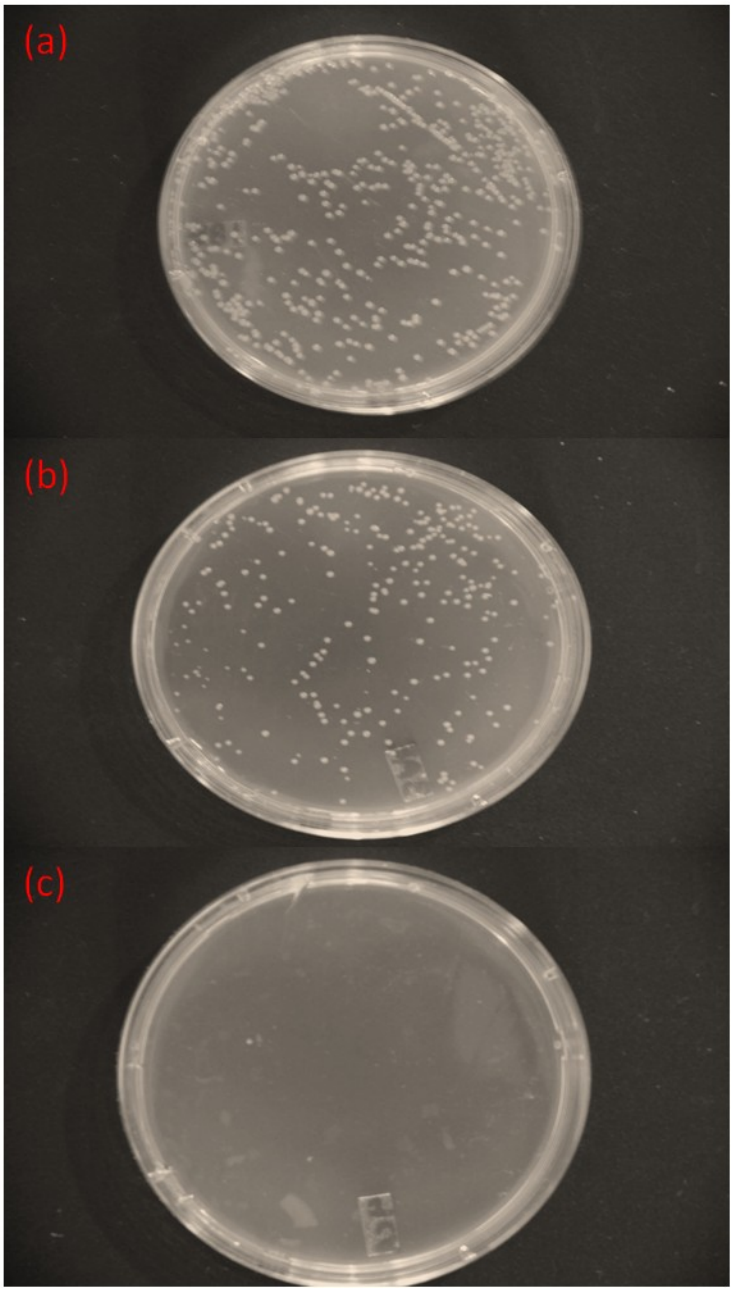

Figure 6.7. a) The fifth dilution (1:100000) of the negative test b) The fifth dilution of antibacterial test using TiO_2 sample. c) The fifth dilution of Ag/TiO_2 sample shows the full inhibition.

To make sure that the nanoparticles stay attached to the nanotubes during the test, we have conducted a separate test. For this, we have left the sample inside the test cultures for a short time (2 minutes) without shaking. Examining the sample showed no antibacterial activities, and the results were the same as the negative control test. Figure 6.8 shows the agar plate of a negative test and an Ag/TiO_2 test after 2 minutes duration. Identical results of both tests confirm no silver diffusion.

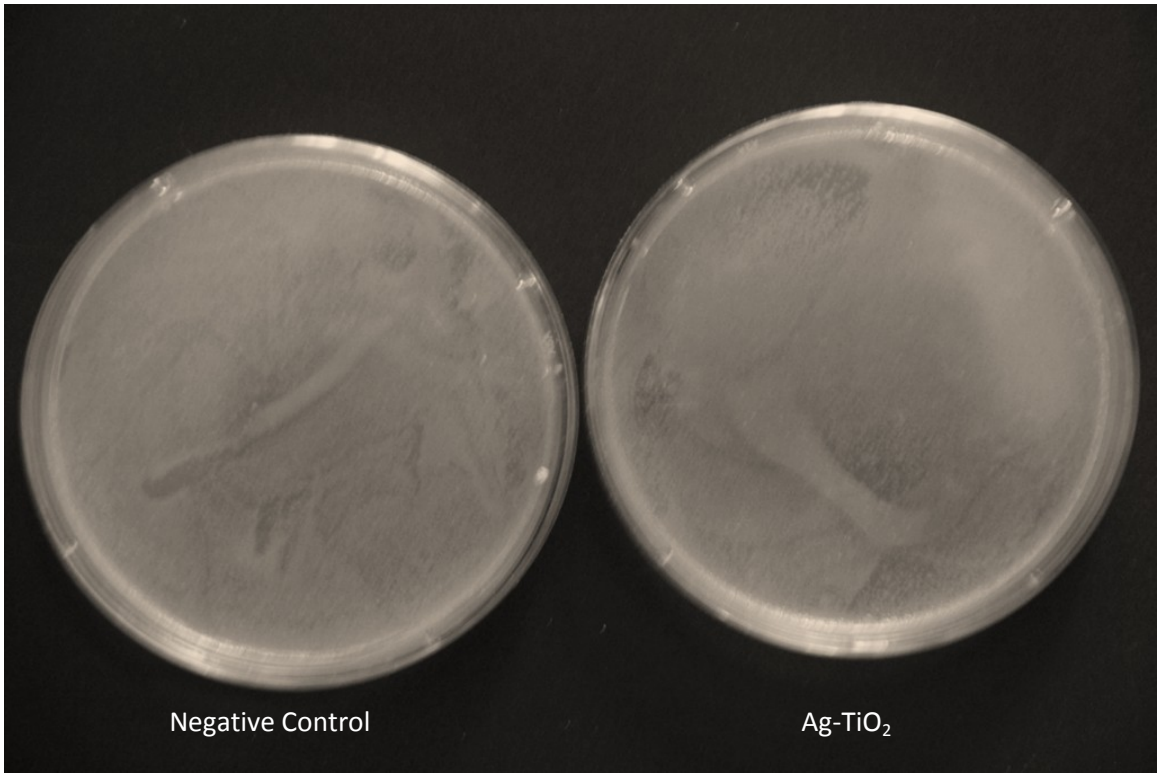

Figure 6.8. Large amounts of bacteria colonies in both cases confirm no silver diffusion from nanotubes samples.

The above observations shows that silver nanoparticles do not disperse during the test and the full inhibition might be because of silver abundance on the sample surface.

In the following, the tests were done on the samples with lower amount of silver nanoparticles (the duration of silver electrodeposition was about 5 minutes).

Figures 6.9, 6.10 and 6.11 illustrate a comparison between the triplications of the last dilution of Negative control, Titania film and silver modified Titania tests. The test culture was made of 50µL overnight bacteria culture and 950µL LB to make the colonies of fifth dilution easier to count. The small variation among the replication results validates the test accuracy.

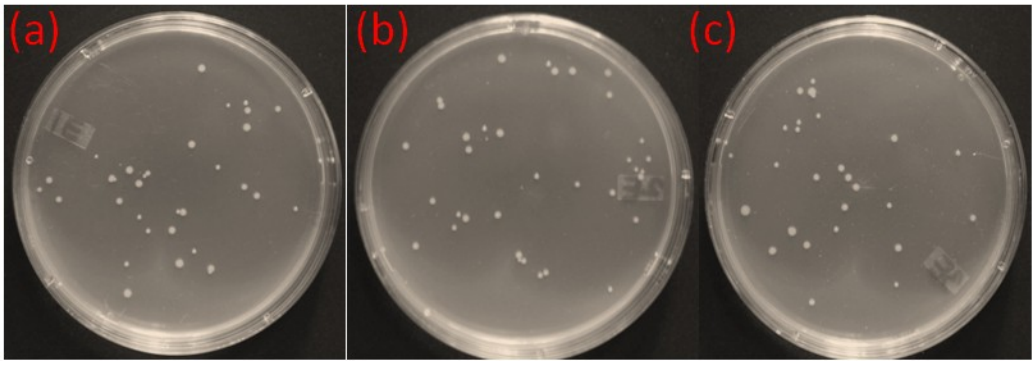

Figure 6.9. Triplications of negative test containing 32, 36 and 27 colonies. The small variation among the results validates the test accuracy.

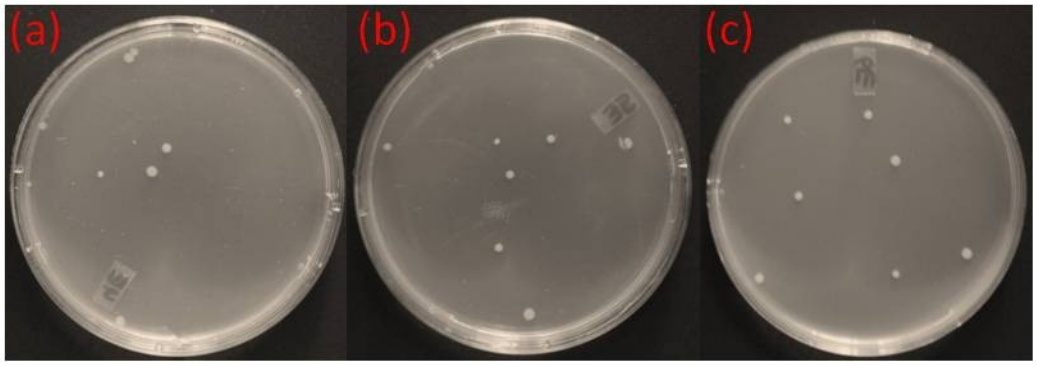

Figure 6.10. Triplications of TiO2 sample containing 8, 7 and 7 colonies.

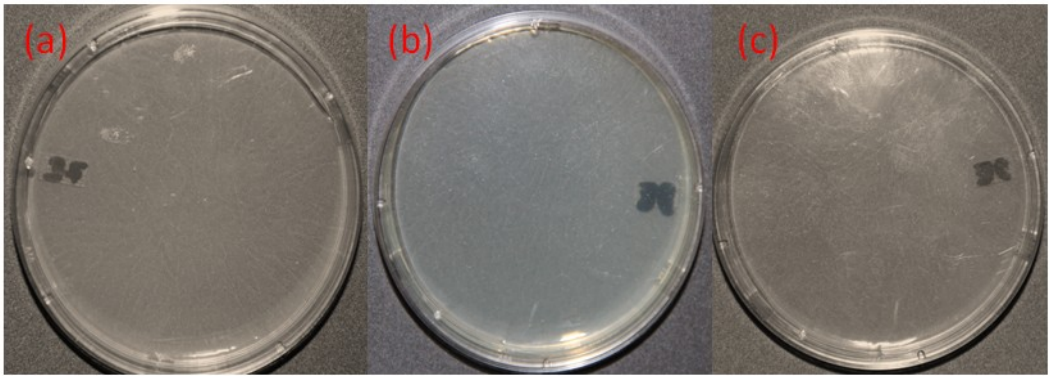

Figure 6.11. Full inhibition of Ag/TiO_2 sample

All the test results such as number of colonies, standard deviation of the replications and bactericidal efficiency of the samples are summarized in Table 6.1. The number of survived colonies before dilutions are considered (calculated from the fifth dilution multiplying by 10^5).

Sample	Number of colonies $\times 10^5$	Antibacterial efficiency
Negative Control	320±4.5	------
TiO_2	70±0.57735	78%
Ag/TiO_2	0	100%

Table 6.1. Antibacterial efficiency according to the number of colonies

Chapter 7: Conclusion, contributions and future works

7.1 Summary of the thesis

In this research we have investigated design, and fabrication of Ag/TiO_2 nanotubes. The fabricated nanostructure was used to eliminate E-coli bacteria. The combination of Titanium dioxide and silver nanostructures, showed a very strong effect in inhibition of bacteria since they had exhibited their germicidal effects individually.

The accomplished targets in fabrication and application of the nanostructure are as follow:

- Titanium dioxide nanotube arrays were fabricated through an anodization process.
- The effective parameters were monitored to optimize titanium dioxide nanotubes.
- A doping process was performed to increase the conductivity to be prepared for an electrodeposition procedure.
- Silver was electrodeposited on Titanium dioxide nanotube film using a three electrode chemical cell.
- Antibacterial effect of the samples were determined in a liquid media test against E.Coli

To the best of our knowledge, this is the first time that uniformly-deposited silver on TiO_2 array of nanotubes is fabricated and used for antibacterial applications.

7.2 Suggestions for Future works

In this research TiO_2 nanotubes fabricated in ambient temperature (22˚C) it could draw your attention to examine the fabrication in higher temperatures and check the effects on its conductivity as it is an important issue for depositing silver into the pores. Weather if annealing improves silver deposition, can also be verified.

This research proved antibacterial activity of the prepared device with anodization and deposition durations instead of considering the exact amount of anodized TiO_2 and Ag nanostructures. Evaluation the exact amount of TiO_2 and Ag before antibacterial test helps to calculate the exact bacterium inhibition efficiency.

TiO_2 membranes prepared by opening the tube bottoms with a controlled diameter can be applied in water purification systems while having antibacterial effect simultaneously.

References

[1] Estimated with data from WHO/UNICEF Joint Monitoring Programme (JMP) for Water Supply and Sanitation. (2012). Progress on Sanitation and Drinking-Water, 2012 Update.

http://www.who.int/water_sanitation_health/publications/2012/jmp_report/en/

[2] M.A. Shannon, P.W. Bohn & M.Elimelech, "Science and technology for water purification in the coming decades," *Nature London*, vol. 452, no. 7185, pp. 301–310, 2008.

[3] N. Savage & M.S. Diallo, "Nanomaterials and water purification: Opportunities and challenges," *J. Nanoparticle Research*, vol. 7, pp. 331–342, May.2005.

[4] M. De Kwaadsteniet, M. Botes & T.E. Cloete, "Application of nanotechnology in antimicrobial coatings in the water industry," *World Scientific*, vol. 6, no. 5, pp. 395–407, Jun.2011.

[5] http://en.wikipedia.org/wiki/Biofouling 09/04/2013

[6] J. Theron, J.A. Walker & T.E. Cloete, "Nanotechnology and water treatment: applications and emerging opportunities," *Critical Reviews in Microbiology*, vol. 34, no. 1, pp. 34–43, 2008.

[7] D.K. Tiwari, J. Behari & P.Sen, "Application of Nanoparticles in Waste Water Treatment," *World Applied Science J*., vol. 3, pp. 417–433, 2008.

[8] http://www.eolss.net/Sample-Chapters/C07/E6-144-23.pdf
El Saliby, I. J., Shon, H. K., Kandasamy, J., & Vigneswaran, S. NANOTECHNOLOGY FOR WASTEWATER TREATMENT: IN BRIEF

[9]E.V. Skorb, L.I. Antonouskaya & N.A. Belyasova, "Antibacterial activity of thin-film photocatalysts based on metal-modified TiO2 and TiO2:In2O3 nanocomposite," *Applied Catalysis B:* Environmental, vol. 84, pp. 94–99, 2008.

[10] S.D. Mo & W.Y. Ching, "Electronic and optical properties of three phases of titanium dioxide: Rutile, anatase, and brookite," *Physical Rev.* B, vol. 51, no. 19, pp. 13024–13032, Nov.1994.

[11] Smyth, J. (2011). TiO2 Structure. Retrieved October 15, 2012 from University of Colorado, Web site: http://ruby.colorado.edu/~smyth/min/tio2.html

[12] U. Diebold, "Structure and properties of TiO2 surfaces: a brief review," *Applied Physics a Materials Science and Processing*, vol. 76, no. 5, pp. 681–688, Oct.2002.

[13] P. Hoyer, "Formation of a Titanium Dioxide Nanotube Array," *Langmuir*, vol. 12, no. 6, pp. 1411–1413, Dec.1995

[14] P. Roy, S. Berger & P.Schmuki, "TiO2 Nanotubes: Synthesis and Applications," *Angewandte Chemie*, vol. 50, no. 13, pp. 2904–2939, 2011.

[15] J.M. Macak, H. Tsuchiya & A.Ghicov, "TiO2 nanotubes: Self-organized electrochemical formation, properties and applications," *Current Opinion in Solid State and Materials Science*, vol. 11, no. 1, pp. 3–18, Aug2007.

[16] V. Zwilling, E.D. Ceretti & A.B. Forveille, "Structure and Physicochemistry of Anodic Oxide Films on Titanium and TA6V Alloy," *Surface and Interface Analysis*, vol. 27, no. 7, pp. 629–637, 1999.

[17] V. Zwilling, M. Aucouturier & E.D. Ceretti, "Structure and Physicochemistry of Anodic Oxide Films on Titanium and TA6V Alloy," *Electrochimica Acta*, vol. 45, no. 6, pp. 921–929, Jun.1999

[18] M. Macak, K. Sirotna & P.Schmuki, "Self-organized porous titanium oxide prepared in Na2SO4/NaF electrolytes," *Electrochimia Acta*, vol. 50, pp. 3679–3684, Jan-2005.

[19] S. P. Albu., A. Ghicov & J. M. Macak. "250 µm long anodic TiO2 nanotubes with hexagonal self-ordering." *physica status solidi (RRL)-Rapid Research Letters 1*, no. 2 (2006): R65-R67

[20] M. Paulose, K. Shankar & S.Yoria, "Anodic Growth of Highly Ordered TiO2 Nanotube Arrays to 134 ím in Length," *The J. Physical Chemistry B*, vol. 110, pp. 16179–16184, Sep.2007.

[21] H. Tsuchiya, J.M. Macak & L.Taveira, "Self-organized TiO sub 2/sub nanotubes prepared in ammonium fluoride containing acetic acid electrolytes," *Electrochemistry Comm*., vol. 7, no. 6, pp. 576–580, Apr.2005.

[22] J.M. Macak & P. Schmuki, "Anodic growth of self-organized anodic TiO2 nanotubes in viscous electrolytes," *Electrochimica Acta*, vol. 52, no. 3, pp. 1258–1264, Aug2006.

[23] B.G. Lee, J.W. Choi & S.E. Lee, "Formation behavior of anodic TiO2 nanotubes in fluoride containing electrolytes," *Transaction of Nonferrous Metals Society of China*, vol. 19, pp. 842–845, Mar.2009

[24] G.K. Mor, O.K. Varghese & M.Paulose, "A review on highly ordered, vertically oriented TiO2 nanotube arrays: Fabrication, material properties, and solar energy applications," *Solar Energy Materials & Solar Cells*, vol. 90, no. 14, pp. 2011–2075, Apr.2006.

[25] A. Watcharenwong & W. Chanmanee, "Self-organized TiO2 nanotube arrays by anodization of Ti substrate: Effect of anodization time, voltage and medium composition on oxide morphology and photoelectrochemical response," *J. Materials Research*, vol. 22, no. 11, pp. 3186–3195, Nov.2007.

[26] D. Gong, C.A. Grimes & O.K. Varghese, "Titanium oxide nanotube arrays prepared by anodic oxidation," *J. Materials Research*, vol. 16, no. 12, pp. 3331–3334, Sep.2001.

[27] S. Sakthivel, M.V. Shankar & M.Palanichamy, "Enhancement of photocatalytic activity by metal deposition: characterization and photonic efficiency of Pt, Au and Pd deposited on TiO2 catalyst," *Water Research*, vol. 38, no. 13, pp. 3001–3008, Apr. 2004.

[28] M. Macak, B.G. Gong & M.Hueppe, "Filling of TiO2 Nanotubes by Self-Doping and Electrodeposition," *Advanced Materials*, vol. 19, no. 19, pp. 3027–3031, 2007.

[29] I. Paramasivam, J.M. Macak & P.Schmuki, "Photocatalytic activity of TiO2 nanotube layers loaded with Ag and Au nanoparticles," *Electrochemistry Comm*., vol. 10, pp. 71–75, Nov.2007.

[30] M. De Kwaadsteniet, M. Botes & T.E. Cloete, "Application of nanotechnology in antimicrobial coatings in the water industry," *World Scientific*, vol. 6, no. 5, pp. 395–407, Jun.2011.

[31] J.C. Colmenares, M.A. Aramendia & A.Marinas, "Synthesis, characterization and photocatalytic activity of different metal-doped titania systems," *Applied Catalysis*, vol. 306, pp. 120–127, Mar.2006.

[32] I.M. Butterfield, P.A. Christensen & T.E. Curtis, "WATER DISINFECTION USING AN IMMOBILISED TITANIUM DIOXIDE FILM IN A PHOTOCHEMICAL REACTOR WITH ELECTRIC FIELD ENHANCEMENT," *Pergamon*, vol. 31, no. 3, pp. 675–677, Nov.1996.

[33] J.R. Morones, J.L. Elechiguerra & A.Camacho, "the bactericidal effect of silver nanoparticles," J*. Nanotechnology*, vol. 16, no. 10, pp. 2346–2353, Jul.2005

[34] S.J. Fonash, Solar Cell Device Physics., Oxford: Academic Press, 2010, pp. 295–308.

[35] Rey, G., Consonni, V. & Karst (2009). Dye Sensitized Solar Cells. Retrieved January 1, 2013 from LMGP, Web site: http://www.lmgp.grenoble-inp.fr/recherche/dye-sensitized-solar-cells-289401.kjsp

[36] P. Roy, D. Kim & K.Lee, "TiO2 nanotubes and their application in dye-sensitized solar cells," *Nanoscale*, vol. 2, pp. 45–59, Dec.2009.

[37] E.C. Wells, *Scanning Electron Microscopy*, New York: McGraw-Hill, 1974, pp. 1–2.

[38]http://www2.warwick.ac.uk/fac/sci/physics/current/postgraduate/regs/mpags/ex5/techniques/structural/sem3/ 2013/01/11

[39]http://www.charfac.umn.edu/instruments/hitachi_s-4700_instructions.pdf 11/01/2013

[40] J.W. Gardner & V.K. *Varadan, Microsensors, Mems and Smart Devices*, New York: John Wiley & Sons, 2001, pp. 50–51.

[41] http://ns.kopt.co.jp/English/ca_jou-gi/img/supatter_zu.jpg 11/04/2013

[42]http://en.wikipedia.org/wiki/Energy-dispersive_X-ray_spectroscopy#Equipment 13/01/2013

[43]http://tawadascientific.com/main.php?page=how-xrf-works&lang=in 13/01/2013

[44] Electrochemical Society & F.A. Lowenheim, *Modern electroplating*. 3rd ed., New York: Wiley, 1974, pp. 1–8.

[45] S. Dimitrijev, *Understanding semiconductor devices*, New York: Oxford University Press, 1958, pp. 179–184.

[46] D.A. Neamen, *Semiconductor physics and devices*: basic principles. 3rd ed., Boston: McGraw-Hil, 1992, pp. 326–348.

[47] http://www.cdc.gov/ecoli/general/index.html ^ "Escherichia coli". CDC National Center for Emerging and Zoonotic Infectious Diseases. Retrieved 2012-10-02

[48] M. Madigan, *Brock biology of microorganisms*. 8th ed., New Jersey : Prentice Hall, 1997, p. 151.

[49] X. Chen & H.J. Schluesener, "Nanosilver: A Nanoproduct in Medical Application," *Toxicology Lett*, vol. 176, pp. 1–12, 2008.